APPLICATIONS GUIDE

Argolight Solutions

Version 1.0
April 2017
www.argolight.com

Table of contents

1. Monitoring fluorescence microscopes: why, what, when and how?

Calibration versus quality control

The term “calibration” is often misused, especially in the field of fluorescence microscopy. It is therefore important to define it precisely, and to discuss the difference between “calibration” and “quality control”.

One the one hand, calibration consists in comparing measurement values delivered by a device being tested with the values of a calibration standard of known accuracy. This implies the use of standards or reference materials, in general from National Metrology Institutes. Having access to a calibrated device allows to perform measurements, in the sense of metrology.
Unfortunately, there is no calibration standards nor reference materials for fluorescence microscopes that would allow to carry out measurements. That is why manufacturers do not sell fluorescence microscopes as metrology tools, but as imaging tools.

On the other hand, quality control consists in determining, by using appropriate tools, if an instrument fulfills quality specifications or pre-established requirements, to insure the reproducibility of its performances within a certain margin. This implies to know or to define these specifications or requirements, and to monitor them over time.

Quality control does not allow to turn a fluorescence microscope from an imaging instrument into a metrology one. However, it enables the comparison of results between two fluorescence microscopes, or the measure of performance fluctuations of one microscope over time.

The term “quality control” is therefore more appropriate than “calibration” for the field of fluorescence microscopy.

Quality control: why?

Fluorescence imaging has become ubiquitous in life sciences laboratories, including those focused on pharmaceuticals, diagnosis, and forensics.
In life sciences experiments, two main sources of error are possible: errors coming from the sample preparation, and those coming from the imaging system. Controlling regularly the quality of such instruments allows to remove the bias they introduce on life sciences experiments.

Modern fluorescence imaging systems are complex instruments made of many optical, mechanical, and electronical components. The possibilities of misalignment, malfunction or failure of such instruments increase with the number of components.

For example, laser-scanning microscopes (confocal, spinning disk, etc.) tend to fluctuate more than widefield microscopes, simply because they have more components (such as piezo stages, galvo mirrors, lasers, and photomultiplier tubes) that are subject to change [1].

The different actors involved in the field of fluorescence microscopy can mutually benefit from controling the quality of such instruments:

- Manufacturers: insure instruments' specifications and prevent disagreements with customers (sample versus instrument).
- Core facilities: insure instruments' level of performances compatible to the users' expectations, prevent disagreements with users (sample versus instrument), anticipate instrument failure and reduce machine downtime.
- For users: insure the acquisition of reliable data, remove the bias introduced by the instrument, know how the system performances evolve over time, and perform quantitative microscopy.

Quantitative microscopy is very important for the scientific community as it makes it possible to compare studies performed at different times, at different places, and from different instruments [2,3].

Quality control: what?

There are many aspects to quality-control in a fluorescence microscope.
In an article published in 2005 [4], the Federal Institute for Materials Research and Testing, a German Metrology Institute, has listed the main parameters, among many others, that would be desired to characterize:
"The size of the illuminated volume, i.e. the point-spread function, the instrument's spatial (x, y) resolution, the spectral irradiance/excitation intensity reaching the sample, the homogeneity of the sample illumination, the field flatness, z-distance and z-resolution, the spectral resolution as well as the day-to-day and long-term instrument performance."

Quality control: when?

Many factors will determine how often the quality of a fluorescence microscope should be controlled:

- the type of instrument (widefield versus confocal),
- its components (mercury or metal-halide lamp versus more stable LEDs),
- the experience of the user (an experienced microscopist will notice changes more readily than a novice),
- whether the system is shared,
- the type of experiment for which it is used,
- the level of quality needed.

For example, a researcher carrying out a single experiment would not need to monitor performance but simply to know that the system performs well. On the contrary, someone who needs to perform multiple experiments at different times would have to know the system's fluctuations to compare data.

It may not be realistic to control all the above-mentioned aspects before each imaging session. However, depending on the study, some of them need to be assessed.
Simple examples are the control of the objective status before any imaging session, the control of chromatic aberrations before colocalization studies, the control of the system's intensity response before any experiment where intensity is meant to be used, etc.

A deeper control can take place just after the installation of a new system or after a maintenance. A reference status of the system performances can then be defined: a point to go back for comparison if needed, each time the system is assessed.

Thus, manufacturer specifications can be validated and system's performances monitored over time.
Assessing periodically a fluorescence microscope enables to quickly identify and solve microscope issues. This would prevent the acquisition of corrupted data, and the consequent question: since when the data generated by the microscope have been corrupted? It also minimizes machine downtime by optimizing maintenance, not based on a subjective image of a biological sample, but on objective and quantified parameters.

Quality control: how?

Many existing tools, with different relevancies and performances, can be used to control the fluorescence microscopes' quality: beads, plastic slides, resolution targets, reticles, thin layers, etc. The description of these tools, their properties and their respective advantages and drawbacks are not within the scope of this document.

However, whatever the chosen tools, they must respect at least two criteria:

- The elements/patterns composing the tool must be fluorescent. This sounds obvious, but tools presenting elements that show a contrast other than fluorescence, such as absorption or refractive index, are not suited to assess fluorescence imaging systems.
- The fluorescent elements/patterns should be placed after a microscope coverslip with a thickness of (170±5) µm and a refractive index at 546 nm of 1.5255±0.0015. The thickness and refractive index of microscope coverslips are standardized through the ISO 8255-1 norm. By doing so, the imaging conditions, for which coverslip-corrected microscope objectives are designed, are respected.

Argolight multidimensional tools are specifically designed for the quality control (alignment, performances assessment, validation and monitoring) of fluorescence imaging systems (wide-field, confocal, spinning disk, structured illumination, etc.).
They are composed of different fluorescent patterns in two and three dimensions, as well as analysis algorithms extracting relevant parameters about the microscope status from images of these patterns.
Argolight tools contain fluorescent patterns positioned 170 µm deep inside the glass, presenting the same refractive index as microscope coverslips. These conditions, for which coverslip-corrected microscope objectives are designed, are perfectly suited to align the different elements (objectives, stages, filters, cameras, etc.) of a fluorescence microscope and to assess its performances.

Scope of this document

The properties and patterns of the current Argo-HM, Argo-LM and Argo-SIM tools are described in the associated User Guides.
The fluorescent patterns they contain can be used to align a fluorescence microscope, to assess and valid its performances, and to follow them over time.
This document presents non-exhaustively different applications for each individual pattern. Some applications can already be managed with Daybook, the image processing software by Argolight, others with human vision- or software-assisted tools.

Quality control is often perceived as a tedious and not rewarding task. Argolight tools aim at keeping this task as simple and quick as possible. Current and further hardware and software developments at Argolight go in this direction.

2. Target (Argo-HM and -SIM)

2.1 Spatial Scaling

Issue

In most microscopes, the size of the field of view is theoretically determined from the objectives' and other lenses' magnification, camera chip size (for systems having cameras) and zoom magnification (for laser scanning systems).
Because these parameters can be inaccurate, the practical size of the field of view may differ from the theoretical one.

The actual size of the field of view can be checked with a pattern of known dimensions.

Example

Figure 1 shows confocal microscopy images of the target with scale bars measuring the diameter of concentric circles, allowing to check the correctness of the theoretical size of the field of view.

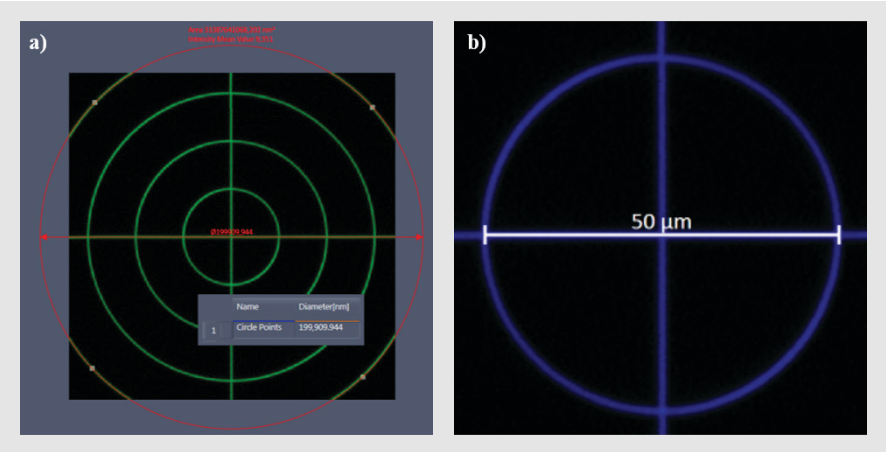

Figure 1: Argo-HM; Confocal microscopy images of the target. Measure the diameter of concentric circles with scale bars to check the correctness of the theoretical size of the field of view.

2.2 Parfocality and parcentrality

Issue

Parfocality and parcentrality are the ability of an instrument to keep an object in the same focus and the same lateral position, respectively, when objectives are switched.

Fine-tuning of instrument parts (objectives, translation stages, filters, etc.) may compensate defects of parfocality and parcentrality, allowing to interchange objectives without readjusting the instrument. In most microscopes, parcentrality cannot be corrected. Parfocality can be compensated by readjusting the Z-stage position, in order to place the sample at the focus.

Parfocality and parcentrality compensations should be performed at the installation or the maintenance of a microscope by an experienced technician.

Procedure to compensate defects of parfocality between different objectives:

- Define the reference focus using the dry objective that has the highest numerical aperture.
- Switch to dry objectives from high numerical apertures to low numerical apertures. Compensate for the focus difference using the Z-stage for each objective.
- Switch to immersion objectives after putting a drop of immersion medium on the sample. Compensate for the focus difference using the Z-stage.

Note: it is important not touching nor changing the sample position while performing this procedure.

Example Figure 2 displays wide-field microscopy images of the target acquired with three different objectives, evidencing defects of parfocality and parcentrality, mainly for the oil objective.

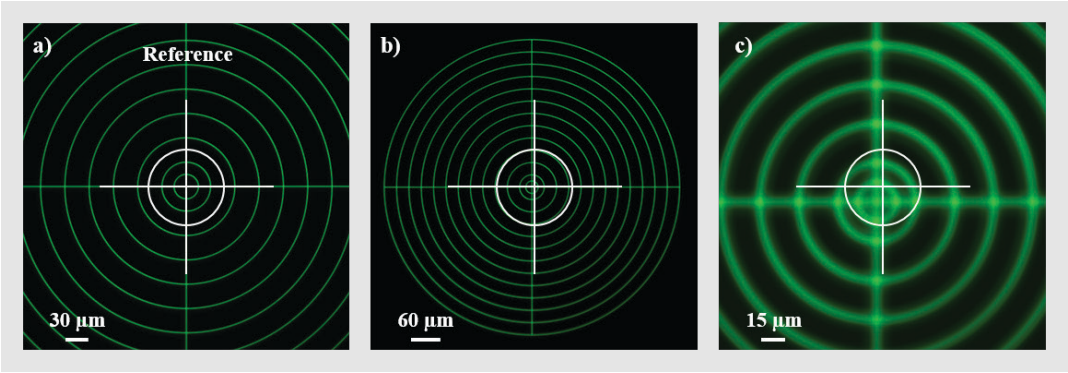

Figure 2: Argo-HM; Wide-field microscopy images of the target on the GFP channel with three different Plan-Apochromat objectives, (a) 40×/0.95 dry, (b) 20×/0.8 dry and (c) 63×/1.4 oil, set on the same turret. The Plan-Apochromat 40×/0.95 dry objective is the reference one.

2.3 Camera alignment

Issue In microscopes using cameras, the alignment of the cameras with respect to the translation stages is important, especially for stitching experiments.

A quick and accurate camera alignment can be achieved easily by using the target.

Example Figure 3 shows wide-field microscopy images of the target, with the camera of the microscope misaligned with respect to the stages, and with the camera well aligned. This application stands also for laser-scanning microscopes, for which the scanning can be oriented accurately with respect to the stages.

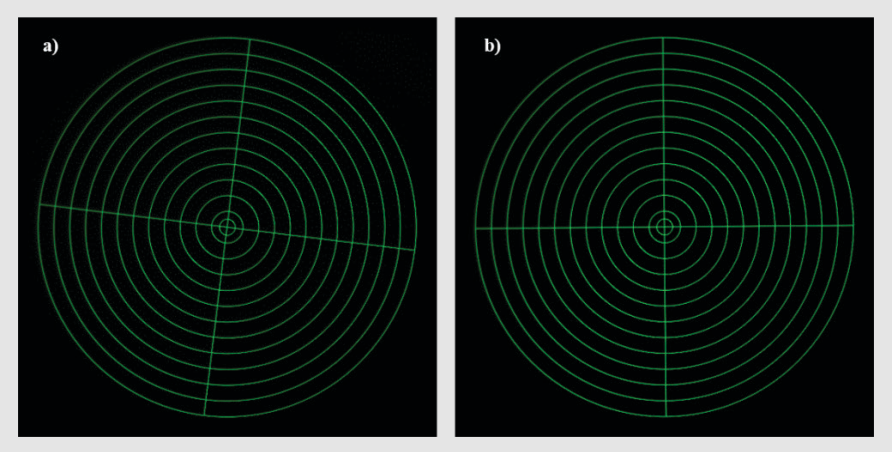

Figure 3: Argo-HM; Wide-field microscopy images of the target, acquired with a 20×/0.8 Plan-Apochromat dry objective on the GFP channel, with (a) the camera misaligned and (b) with the camera aligned with respect to the translation stages.

2.4 Stitching behavior

Issue

Stitching of several images requires first a good alignment (see section 1.3) of the camera (for systems having cameras) or the scanning (for laser-scanning systems) with respect to the translation stages.
Stitching algorithms and associated parameters can be tested, by acquiring several images of different parts of the target, and reconstructing the entire structure.

Inaccurate reconstruction provides information either on:

- the ability of the algorithms to stitch images correctly,
- the non-suitability of the stitching parameters,
- the wrong orientation of the camera (flip, rotate, mirror).

Example

Figure 4 shows stitched images of the target, with inappropriate and appropriate stitching parameters.

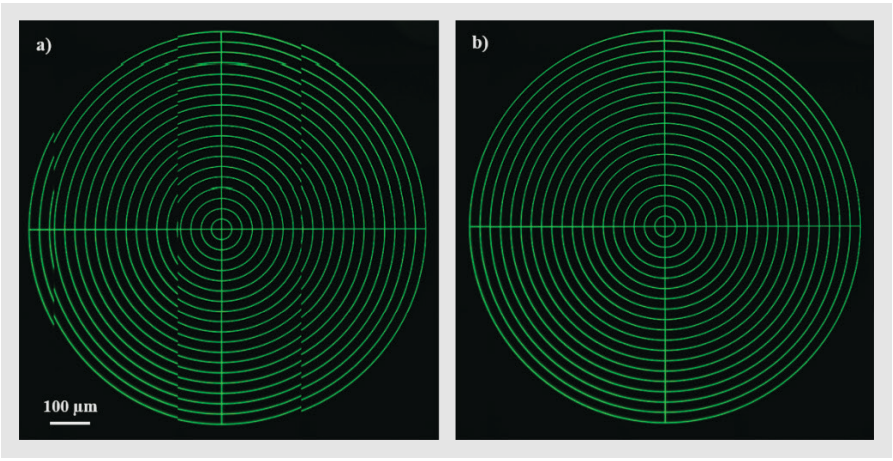

Figure 4: Argo-HM; Wide-field microscopy stitched images of the target, acquired with a 40×/0.95 Plan-Apochromat objective on the GFP channel, with (a) inappropriate and (b) appropriate stitching parameters.

2.5 Alignment of different channels

Issue In systems using several cameras, the alignment of the different channels is crucial to prevent spatial shifts (coming from the instrument) in the acquired images. These shifts can lead to misinterpretations for a biological sample. The target can be used to align one channel with respect to another.

2.6 Scanning rotation

Issue In laser-scanning microscopes, scanning rotation may not perform precisely.

The two perpendicular lines of the target can be used to measure the actual amount of rotation.

Example Figure 5 shows confocal microscopy images of the target, for 0° and 45° scanning rotations. An artificial red square, drawn in the acquisition software along the perpendicular lines of the target, allows to check if the amount of rotation is correct.

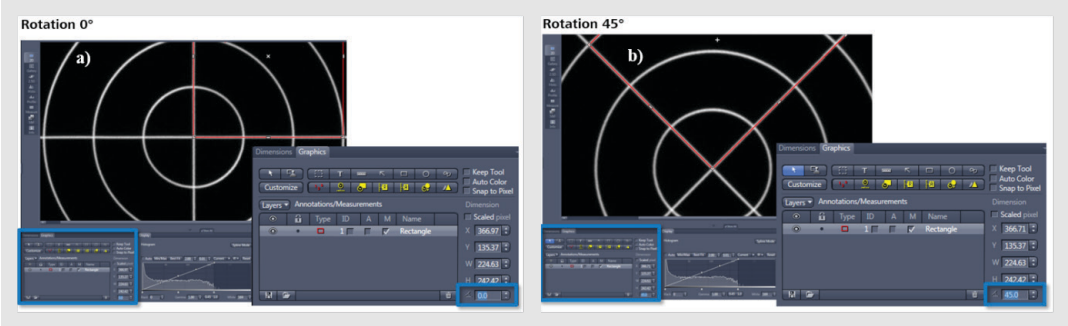

Figure 5: Argo-HM; Confocal microscopy images of the target, (a) with no scanning rotation and (b) with a 45° scanning rotation. An artificial red square at 0° and 45° allows to check if the amount of rotation is correct.

2.7 Scanning performances

Issue In laser-scanning microscopes, scanners used in the bidirectional mode may not maintain the adjustment of the phase between one way and the opposite one.

Example Figure 6 shows confocal microscopy images of a line of the target acquired with the scanning in the monodirectional and bidirectional modes. In the bidirectional mode, a bad adjustment of the phase between one way and the opposite one distorts the image.

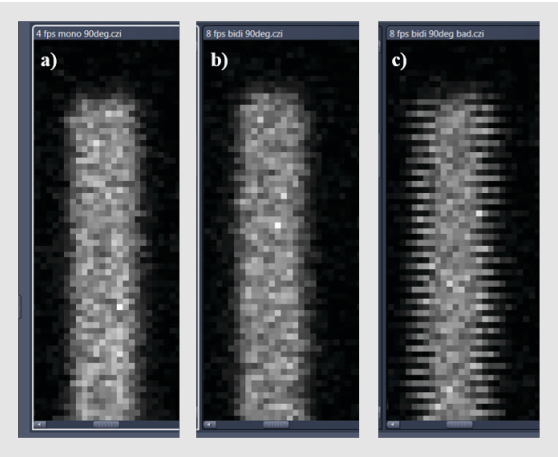

Figure 6: Argo-HM; Confocal microscopy images of a line of the target, with the scanning (a) in the monodirectional mode at 4 frames per second and in the bidirectional mode at 8 frames per second with the round trip (b) in phase and (c) out of phase.

2.8 Optical axis determination

Issue In laser-scanning microscopes, the optical axis of the system can be at a different position with respect to the center of the provided images.
This is due to a misalignment of the system, usually caused when the environment fluctuates or when the laser-confocal-scanning unit undergoes a mechanical shock. As a result, if the misalignment is severe, optical aberrations originally constrained outside the acquired images may appear or be more pronounced.

Example Figure 7 shows confocal microscopy images of the target, not aligned on the center of the field of view, for different scanning orientations. The center of an artificial circle passing through each center of the imaged targets corresponds to the optical axis of the system. Observed deviations of the optical axis should trigger an intervention of the maintenance service.

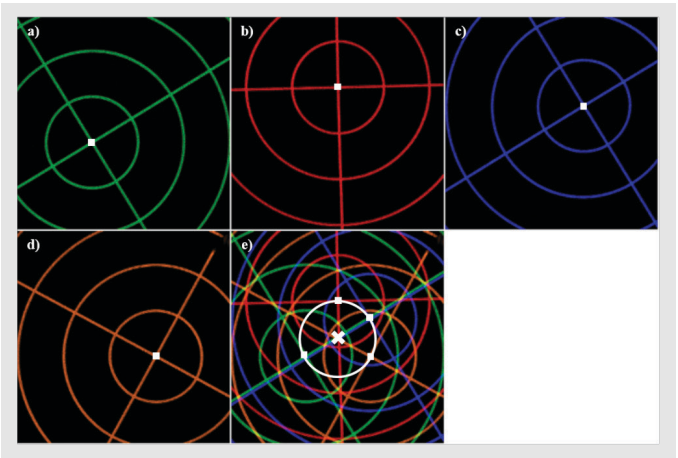

Figure 7: Argo-HM; (a-d) Confocal microscopy images of the target, not aligned on the center of the field of view, for different scanning orientations. (e) Superposition of the images of the decentered target. The center of an artificial circle passing through each center of the imaged targets corresponds to the optical axis of the system.

3. 2D matrix of rings (Argo-HM, -LM and -SIM)

In this section, it is shown how images of a single pattern, a 2D matrix (or field) of rings, acquired on different channels, can lead to the extraction of several parameters of the imaging instrument:

- the homogeneity of the illumination,
- the distortion of the field of view,
- the lateral chromatic shifts,
- the light spreading from lines.

The results provided for each channel are compared and discussed.

Note: The 2D field of rings should be imaged with a lot of care, in order to preserve its function. It is recommended to read carefully the section “Photostability” in the User Guides.

The field of rings from an Argo-HM has been imaged on a laser-scanning confocal microscope. The confocal microscope used for this experiment is recent; it is made available to different users by an imaging facility and is under a maintenance contract.

Images of the field of rings were acquired with the following configuration: 40×/1.3 Plan-Apochromat oil objective, DAPI (λ^{exc} = 405 nm; $\Delta\lambda^{em}$ = 420-460 nm), GFP (λ^{exc} = 488 nm; $\Delta\lambda^{em}$ = 500-540 nm), Texas Red (λ^{exc} = 552 nm; $\Delta\lambda^{em}$ = 570-610 nm) and Cy5 (λ^{exc} = 638 nm; $\Delta\lambda^{em}$ = 650-690 nm) channels, zoom magnification of 2, averaged 8 times. These images are displayed in Figure 8.

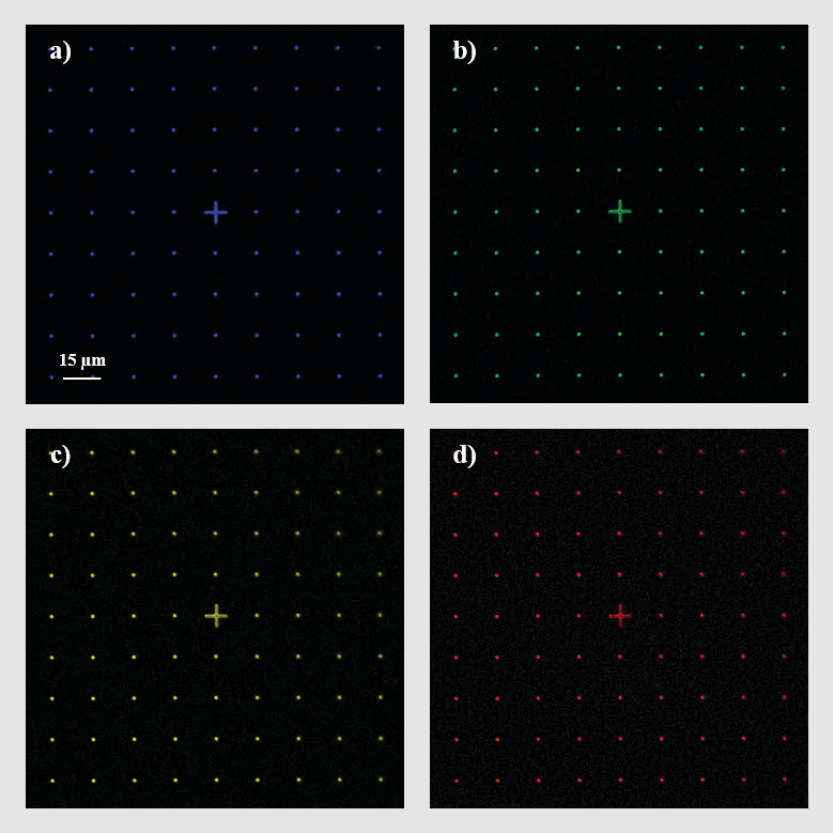

Figure 8: Argo-HM; Confocal microscopy images of the field of rings using a 40×/1.3 Plan-Apochromat oil objective, for the (a) DAPI, (b) GFP, (c) Texas Red and (d) Cy5 channels, zoom magnification of 2, averaged 8 times.

3.1 Homogeneity / uniformity / evenness / flatness of illumination – Shading

Issue

In any fluorescence microscope, the spatial distribution of the illumination intensity is never constant. It is usually maximal in the center of the field of view (if the microscope is well-aligned), and decreases towards the edges, so that a biological sample is never homogeneously illuminated.

The roll-off value* of confocal microscopes should be lower than 20-30%, depending on the manufacturers and the considered systems. The knowledge of the spatial distribution of the illumination intensity onto a sample is therefore important to prevent from misinterpreting intensity differences in images of biological samples.

For information, other appellations than homogeneity can be found in the literature: uniformity, evenness, flatness of illumination, or shading.

Example

From the images of the field of rings shown in Figure 8, Daybook can extract information about the illumination homogeneity.
Figure 9 displays the normalized homogeneity heatmaps. These heatmaps allow to determine the spatial distribution of the illumination, from which different intensity profiles (*cf.* Figure 10), and many parameters (*cf.* Table 1) can be extracted.

Table 1 shows that for all channels, the roll-off value is less than 20% along the purple diagonal, while it is much higher along the pink one.

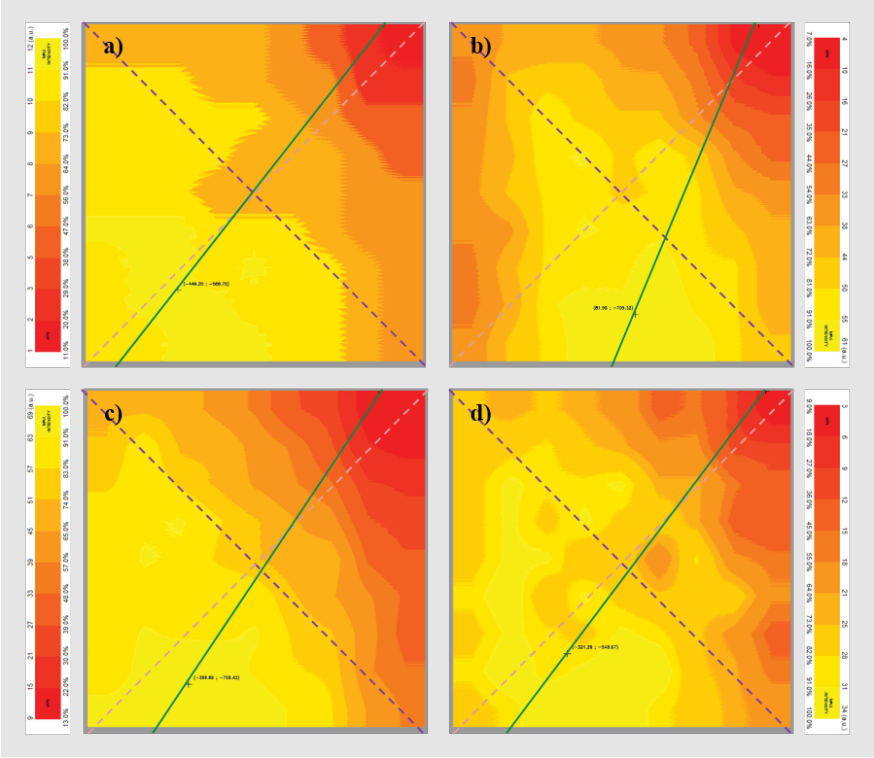

Figure 9: Normalized homogeneity heatmaps for the (a) DAPI, (b) GFP, (c) Texas Red and (d) Cy5 channels. The two small crosses in each heatmap correspond to the maximum and minimum values of the intensity, through which the green line passes.

*Roll-off value: difference between the maximum and the minimum normalized intensity values in the image of a homogeneously fluorescent sample.

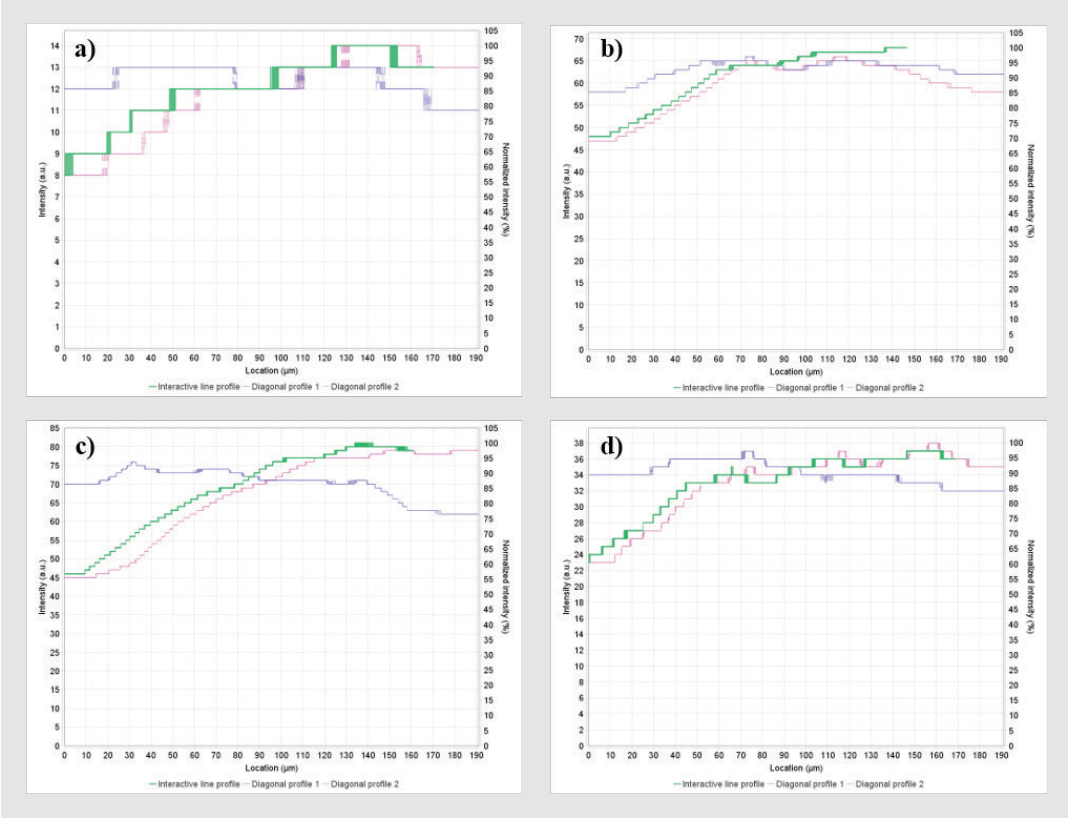

Figure 10: Non-normalized and normalized intensity profiles for the (a) DAPI, (b) GFP, (c) Texas Red and (d) Cy5 channels, along the lines passing through the maximum and the minimum intensities (green line) and along the diagonals (purple and pink dashed lines) of the heatmaps.

Channel	DAPI	GFP	Texas Red	Cy5
Roll-off (%) along the purple diagonal	15.38	12.12	18.42	13.51
Roll-off (%) along the pink diagonal	42.86	28.79	43.04	39.47
X location (µm) of the maximum value	-30.35	5.54	-27.02	-21.71
Y location (µm) of the maximum value	-38.29	-47.93	-49.29	-37.07

Table 1: Some relevant parameters relative to the illumination homogeneity for the DAPI, GFP, Texas Red and Cy5 channels. More information about the meaning and the calculation of these parameters can be found in the documentation of the current version of Daybook.

3.2 Distortion of the field of view

Distortion can be defined as a deformation of the field of view, usually at the corners of an image.

Issue

In any fluorescence microscope, the knowledge of the distortion of the field of view is important when spatial information in an image, such as distances, is aimed to be measured.
Distortion results in spatial variation of the pixel size, *i.e.* the value of the pixel size depends on its location in the field of view. The distortion rate (DR) of microscope objectives is not provided by the manufacturers.

For photography objectives, the distortion is empirically considered to have on the image quality an influence that is:

- negligible if DR < 0.3%,
- weak if 0.3% < DR < 0.4%,
- acceptable if 0.5% < DR < 0.6%,
- large if 0.7% < DR < 0.9%,
- annoying if DR > 1%.

Example

From the images of the field of rings shown in Figure 8, Daybook can extract information about the distortion of the field of view, represented under the form of distortion heatmaps (*cf.* Figure 11).
These heatmaps allow to determine the direction and the magnitude of the distortion through vectors, from which many parameters (*cf.* Table 2) can be extracted.
Table 2 shows that, for all channels, the distortion rate is less than 0.2% along the X axis, while it is less than 0.4% along Y axis.

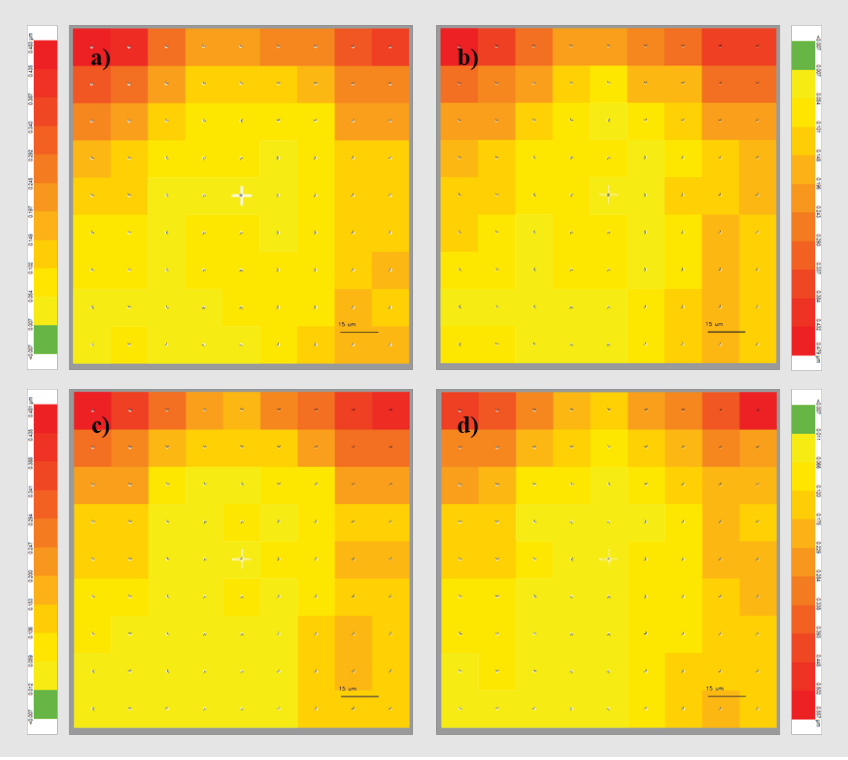

Figure 11: Magnitude and direction heatmaps of the distortion for the (a) DAPI, (b) GFP, (c) Texas Red and (d) Cy5 channels.

Channel	DAPI	GFP	Texas Red	Cy5
Mean vector magnitude (µm)	0.13	0.13	0.13	0.14
Minimum vector magnitude (µm)	0.01	0.01	0.01	0.01
Maximum vector magnitude (µm)	0.48	0.48	0.48	0.56
Maximum distortion rate along X (%)	0.11	0.11	0.06	0.17
Maximum distortion rate along Y (%)	0.34	0.34	0.39	0.40

Table 2: Some relevant parameters relative to the distortion for the DAPI, GFP, Texas Red and Cy5 channels. More information about the meaning and the calculation of these parameters can be found in the documentation of the current version of Daybook.

3.3 Chromatic shifts

Issue

In any fluorescence microscope, the knowledge of the chromatic aberrations, both in the lateral and axial directions, is important when color information in an image is aimed to be used. In particular, for co-localization tests in images of biological samples stained with several labels, chromatic shifts between the different channels must be known and compensated to prevent from misinterpretation.

Microscopes can be corrected for chromatic aberrations, up to a certain extent. For example, objectives and other optical components can be fabricated to have an apochromatic quality. According to microscope manufacturers, apochromatic quality means that, for 4-5 different colors, the chromatic shifts, both lateral and axial, must be less than the system's resolution for the highest wavelength [5].

Theoretical lateral and axial full-width at half-maximum (FWHM) of the point spread function (PSF), for a confocal microscope with a pinhole diameter ≥ 1 Airy unit, are given by the following equations [6]:

$$FWHM_{xy} = \frac{0.51\lambda_{exc}}{NA} \quad (1)$$

$$\text{and } FWHM_{z} = \frac{0.88\lambda_{exc}}{\left(n - \sqrt{n^2 - NA^2}\right)} \quad (2)$$

Where n is the refractive index of the immersion medium, NA the objective numerical aperture, and λ^{exc} the excitation wavelength.

Thus, for a confocal microscope equipped with a 40×/1.3 Plan-Apochromat oil objective, excitation lasers at 405, 488, 552 and 638 nm, and an immersion medium with a refractive index of 1.518, the lateral and axial theoretical FWHMs of the PSF are those displayed in Table 3.

If the actual lateral chromatic shifts are higher than the theoretical lateral FWHMs of the PSF, then the apochromatic correction is not within the specifications.

Excitation wavelength (nm)	405	488	552	638
$FWHM_{xy}$ (µm)	0.159	0.191	0.215	0.250
$FWHM_z$ (µm)	0.485	0.585	0.662	0.765

Table 3: Theoretical lateral and axial full-width at half-maximum (FWHM) of the point spread function (PSF) for different excitation wavelengths.

3.3.1 Lateral chromatic shifts

Example

From the images of the field of rings shown in Figure 8, Daybook can extract information about the lateral chromatic aberrations.

Figures 12, 13 and 14 display the chromatic shift heatmaps for different pairs of channels. These heatmaps allow to determine the direction and the magnitude of the chromatic shifts through vectors, from which many parameters (*cf.* Table 4) can be extracted.

Table 4 shows that, for all pairs of channels, the chromatic shifts are higher than the theoretical lateral FWHMs of the PSF. Therefore, in this example, the apochromatic correction is not within the specifications.

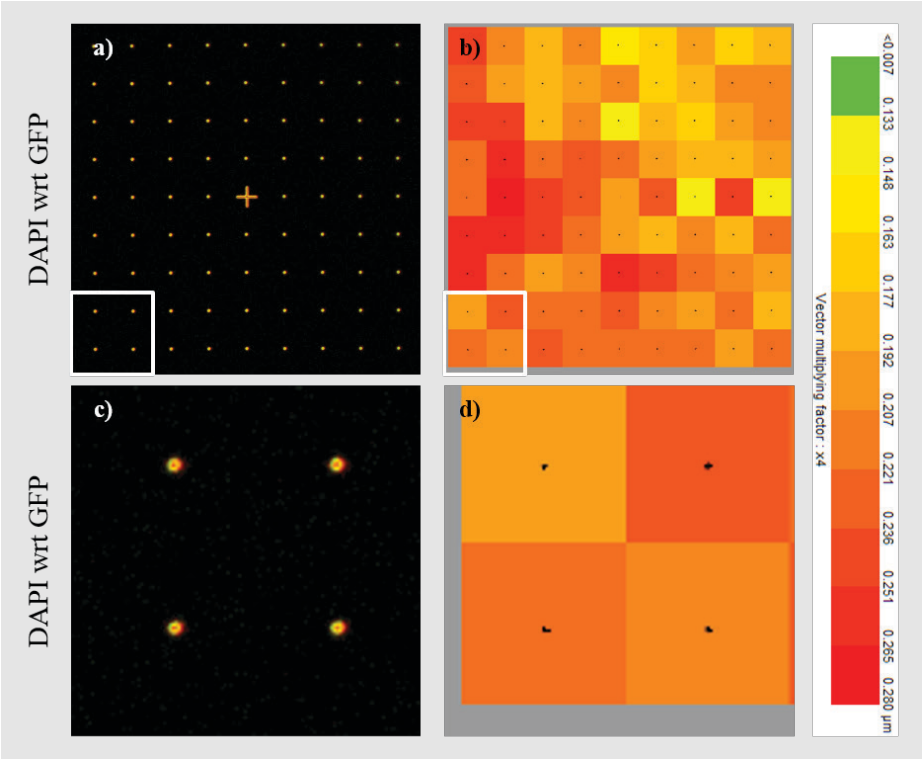

Figure 12: (a, c) Superposition of the confocal microscopy images of the field of rings in the XY plane, for the GFP (in green) and DAPI (in red) channels. (b, d) Corresponding magnitude and direction heatmaps of the chromatic shifts. (c) and (d) are zooms of the left bottom corner of (a) and (b).

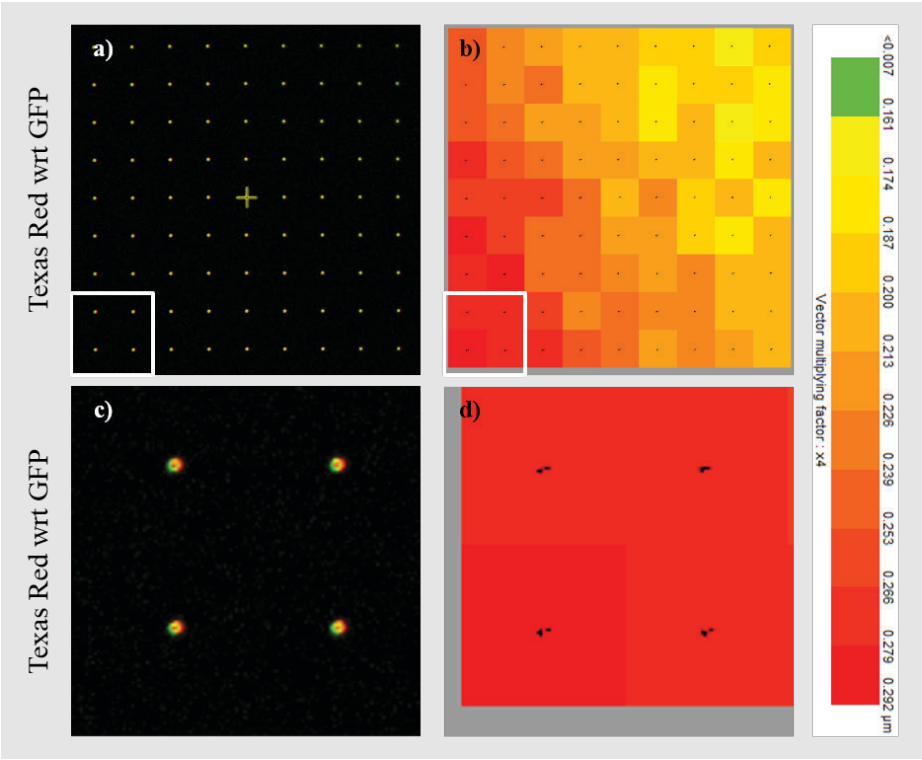

Figure 13: (a, c) Superposition of the confocal microscopy images of the field of rings in the XY plane, for the GFP (in green) and Texas Red (in red) channels. (b, d) Corresponding magnitude and direction heatmaps of the chromatic shifts. (c) and (d) are zooms of the left bottom corner of (a) and (b).

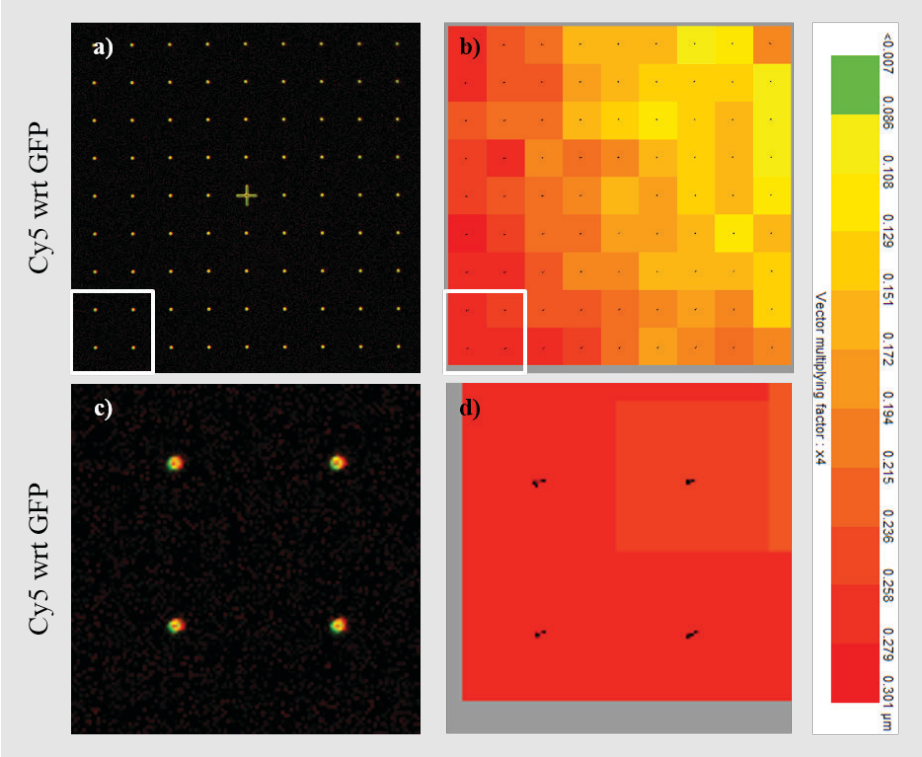

Figure 14: (a, c) Superposition of the confocal microscopy images of the field of rings in the XY plane, for the GFP (in green) and Cy5 (in red) channels. (b, d) Corresponding magnitude and direction heatmaps of the chromatic shifts. (c) and (d) are zooms of the left bottom corner of (a) and (b).

Channel	DAPI wrt GFP	Texas Red wrt GFP	Cy5 wrt GFP
Mean vector magnitude (µm)	0.163	0.229	0.197
Minimum vector magnitude (µm)	0.133	0.161	0.086
Maximum vector magnitude (µm)	0.280	0.292	0.301
Algorithm estimation limit (µm)	0.007	0.007	0.007

Table 4: Some relevant parameters relative to the chromatic shift for the DAPI, GFP, Texas Red and Cy5 channels. More information about the meaning and the calculation of these parameters can be found in the documentation of the current version of Daybook.

3.3.2 Axial chromatic shifts

Example The amount of axial shift due to chromatic aberrations can be determined on the same principle as for lateral shift, as per Figure 15 (wide-field images of the field of rings, both in the XY and XZ planes for the DAPI and GFP channels).

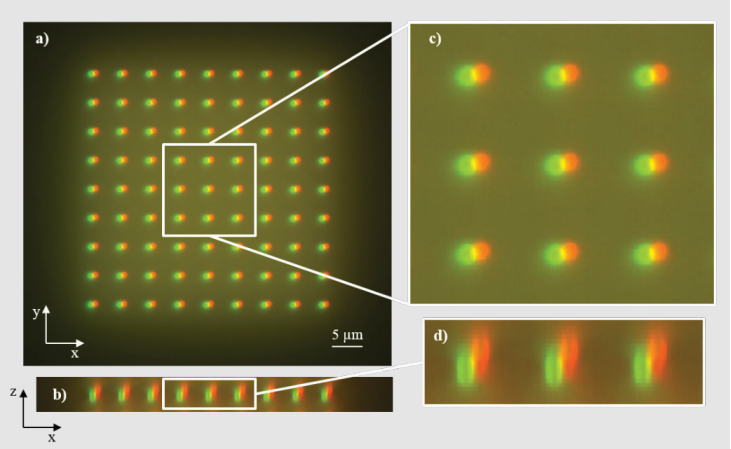

Figure 15: Argo-SIM; Superposition of wide-field microscopy images of the field of rings in the (a) XY and (b) XZ planes, acquired with a 63×/1.4 Plan-Apochromat oil objective for the DAPI (in green) and GFP (in red) channels. (c) and (d) are zooms of (a) and (b). These images show clear chromatic shifts, both in the lateral and axial directions, evidencing that the apochromatic correction is not within the specifications.

3.4 Line spread function

The line spread function test provides information on how and how much the light spreads from a line. The intensity spreading from a line can be modelled with a Gaussian function, which full-width at half maximum (FWHM) informs on the spreading behavior.

The cross inside the field of rings can be used to extract the line spread function in both the vertical and horizontal directions.

Issue

A well-aligned microscope should present symmetric FWHMs, both in the vertical and horizontal directions, for any channel. Besides, according to equation (1) (see page 15), the FWHMs should increase with the excitation wavelength, *i.e.* they should be lower for the DAPI channel than for the Cy5 one.

Example

Figure 16 is a zoom of Figure 8, and shows the cross inside the field of rings for different channels. An intensity line profile is plotted for each channel for both vertical and horizontal directions in Figure 17. A double Gaussian function (sum of two Gaussians) is used to fit the line profiles. Their vertical and horizontal FWHMs are displayed in Table 5.

Results indicate that FWHMs of the Gaussians are larger in the vertical direction that in the horizontal one, for all channels. Besides, the FWHM is the lowest for the GFP channel and the largest for the Texas Red one.

Both these observations indicate that the microscope is not well-aligned.

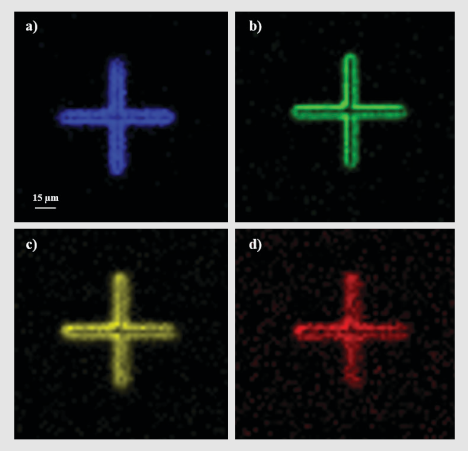

Figure 16: Argo-HM; Zoom showing the cross of the confocal microscopy images of the field of rings using a 40×/1.3 Plan-Apochromat oil objective, for the (a) DAPI, (b) GFP, (c) Texas Red and (d) Cy5 channels, zoom magnification of 2, averaged 8 times.

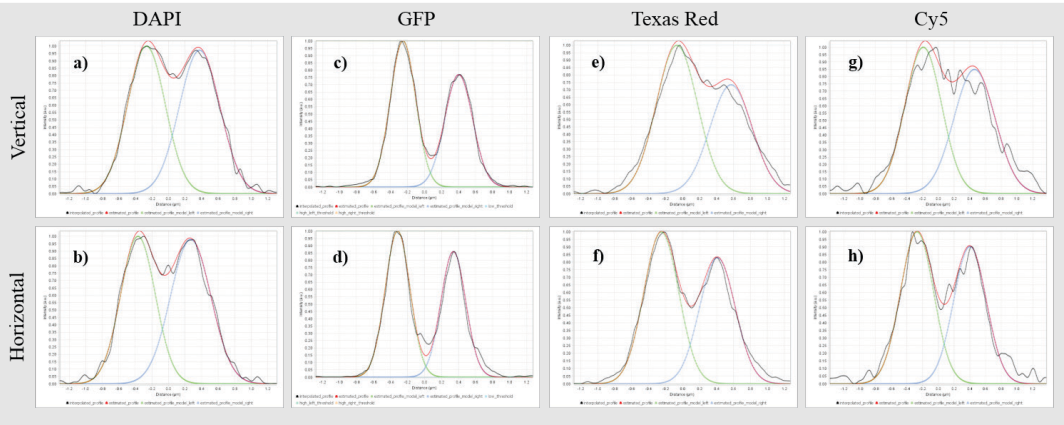

Figure 17: Intensity profiles along the vertical and horizontal directions for the (a, b) DAPI, (c, d) GFP, (e, f) Texas Red and (g, h) Cy5 channels. A double Gaussian function is used to fit the line profiles.

	DAPI		GFP		Texas Red		Cy5	
Direction	Vertical	Horizontal	Vertical	Horizontal	Vertical	Horizontal	Vertical	Horizontal
RMS (a.u.)	0.026	0.032	0.018	0.037	0.050	0.036	0.075	0.056
FWHM (µm)	0.558	0.535	0.369	0.343	0.579	0.489	0.585	0.494

Table 5: RMS and FWHM of the fit functions in the vertical and horizontal directions for the DAPI, GFP, Texas Red and Cy5 channels. A perfect fit has an RMS value of 0. More information about the meaning and the calculation of these parameters can be found in the documentation of the next version of Daybook.

3.5 Comparison of objectives' performances

Issue

Many criteria impact the choice of a microscope objective among several having the same magnification. Besides the numerical aperture, the corrections for optical aberrations are of importance.

Table 6 shows the different objective corrections for the spherical, chromatic and field curvature optical aberrations [5].

Correction for optical aberration	Spherical aberration	Chromatic aberration	Field curvature
Achromat	1 color	2 colors	No
Plan-Achromat	1 color	2 colors	Yes
Semi-Apochromat	2-3 colors	2-3 colors	No
Plan- Semi-Apochromat	3-4 colors	2-4 colors	Yes
Plan-Apochromat	3-4 colors	4-5 colors	Yes

Table 6: Objective corrections for different optical aberrations.

The present study concerns three 10× dry objectives: Plan-Semi-apochromatic 10×/0.3, Plan-Apochromatic 10×/0.45 and Achromatic 10×/0.5. Features of these objectives, including flatness and color correction, provided by the manufacturer's website, are displayed in Table 7.

Note: this study concerns specifically the three objectives that have been made available to us, and cannot necessarily be generalized to all the objectives of these categories.

Objective	Plan-Semi-Apochromatic	Plan-Apochromatic	Achromatic
Magnification	10×	10×	10×
Numerical aperture	0.3	0.45	0.5
Free working distance	5.2 mm	2 mm	1.6 mm
Coverglass thickness	-	0.17 mm	0.17 mm
Flatness	****	*****	*
Color correction	****	*****	*

Table 7: Features of the studied objectives, including flatness and color correction, provided by the manufacturer's website. The number of crosses indicates how good the objective is for the considered feature.

The field of rings has been imaged with these three objectives, mounted on the same wide-field microscope, for the DAPI and GFP channels (*cf.* Figure 18), for the sake of comparing their performances.

Illumination homogeneity (flatness), distortion of the field of view and lateral chromatic (color) correction performances have been evaluated by processing these images with Daybook.

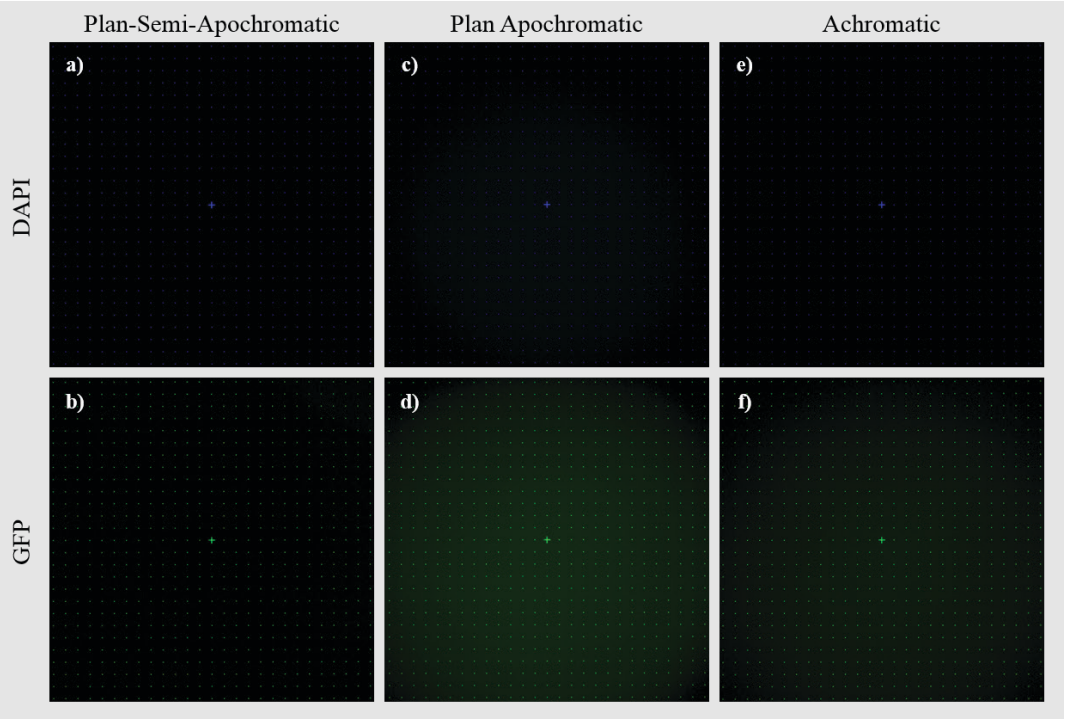

Figure 18: Argo-LM; Wide-field microscopy images of the field of rings using three different 10× dry objectives, (a, b) Plan-Semi-Apochromatic, (c, d) Plan-Apochromatic, and (e, f) Achromatic, for the DAPI and GFP channels.

3.5.1 Flatness of the homogeneity

Example

Figures 19 and 20 display the normalized homogeneity heatmaps and the associated intensity profiles, for the three objectives, DAPI and GFP channels. The relevant parameters associated with the flatness of the homogeneity are gathered in Table 8.

From these figures and table, it can be observed that the maximum of the illumination is better centered in the field of view for the Plan-Apochromatic and the Achromatic objectives. However, the Plan-Semi-Apochromatic objective presents the lowest roll-off value*.

In terms of flatness of the homogeneity, if the roll-off value is the only parameter to consider, the three objectives can therefore be ranked in the following order, from the best to the worst: Plan-Semi-Apochromatic, Plan-Apochromatic and Achromatic.

*Roll-off value: difference between the maximum and the minimum normalized intensity values in the image of a homogeneously fluorescent sample.

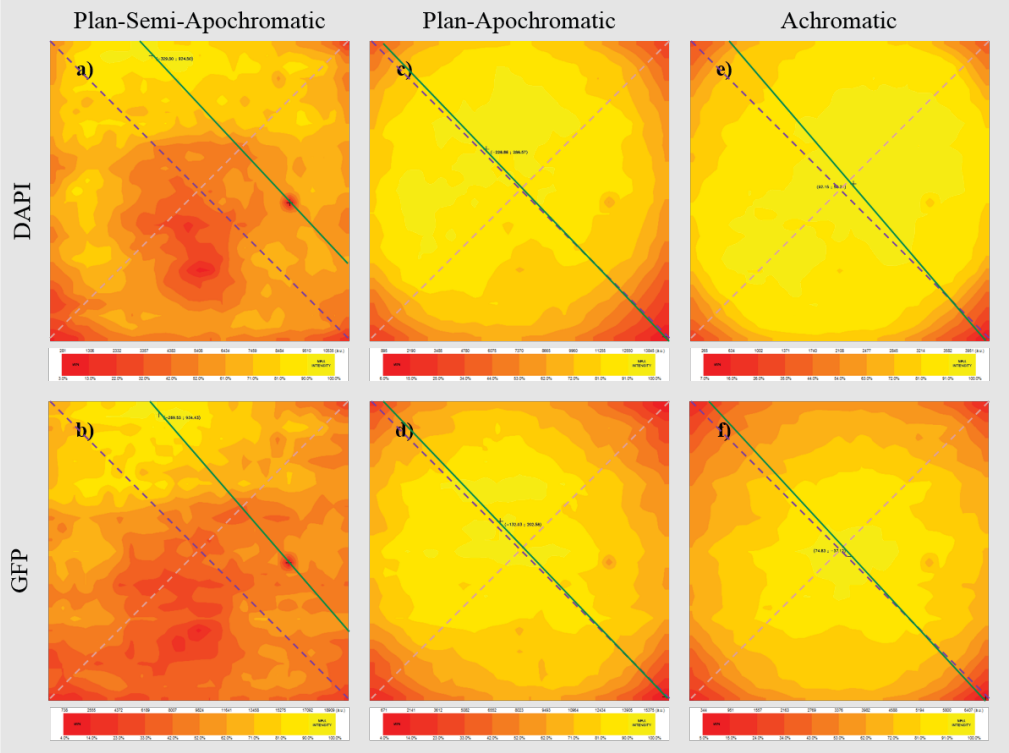

Figure 19: Normalized homogeneity heatmaps for three different 10× dry objectives, (a, b) Plan-Semi-Apochromatic, (c, d) Plan-Apochromatic, and (e, f) Achromatic, for the DAPI and GFP channels. The crosses in the heatmaps correspond to the maximum and minimum values of the intensity.

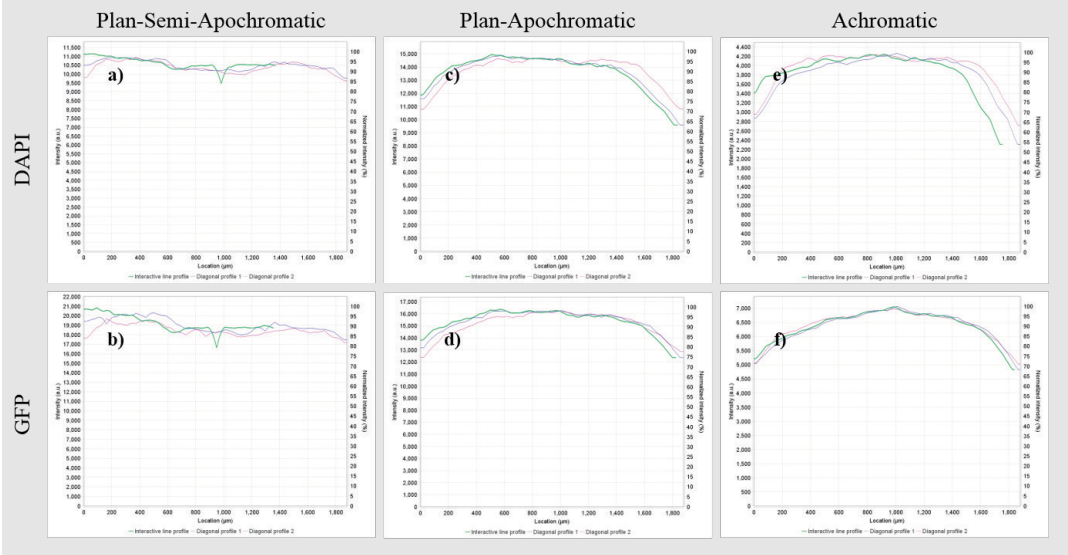

Figure 20: Non-normalized and normalized intensity profiles for three different 10× dry objectives, (a, b) Plan-Semi-Apochromatic, (c, d) Plan-Apochromatic, and (e, f) Achromatic, for the DAPI and GFP channels, along the lines passing through the maximum and the minimum intensities (green line) and along the diagonals (purple and pink dashed lines) of the heatmaps.

	Plan-Semi-Apochromatic		Plan-Apochromatic		Achromatic	
Channel	**DAPI**	**GFP**	**DAPI**	**GFP**	**DAPI**	**GFP**
Roll-off along pink diagonal (%)	10.64	13.95	35.55	23.94	45.81	31.71
Roll-off along purple diagonal (%)	11.93	12.80	26.38	23.64	35.70	27.92

Table 8: Relevant parameters relative to the illumination homogeneity for the three different 10× dry objectives, DAPI and GFP channels. More information about the meaning and the calculation of these parameters can be found in the documentation of the current version of Daybook.

3.5.2 Distortion of the field of view

Example Figure 21 displays the distortion heatmaps for the three objectives, DAPI and GFP channels. The relevant parameters associated with the distortion of the field of view are gathered in Table 9.

From this figure and table, it can be observed that the Plan-Semi-Apochromatic objective presents the lowest distortion rate.

In terms of distortion of the field of view, if the distortion rate is the only parameter to consider, the three objectives can therefore be ranked in the following order, from the best to the worst: Plan-Semi-Apochromatic, Plan-Apochromatic and Achromatic.

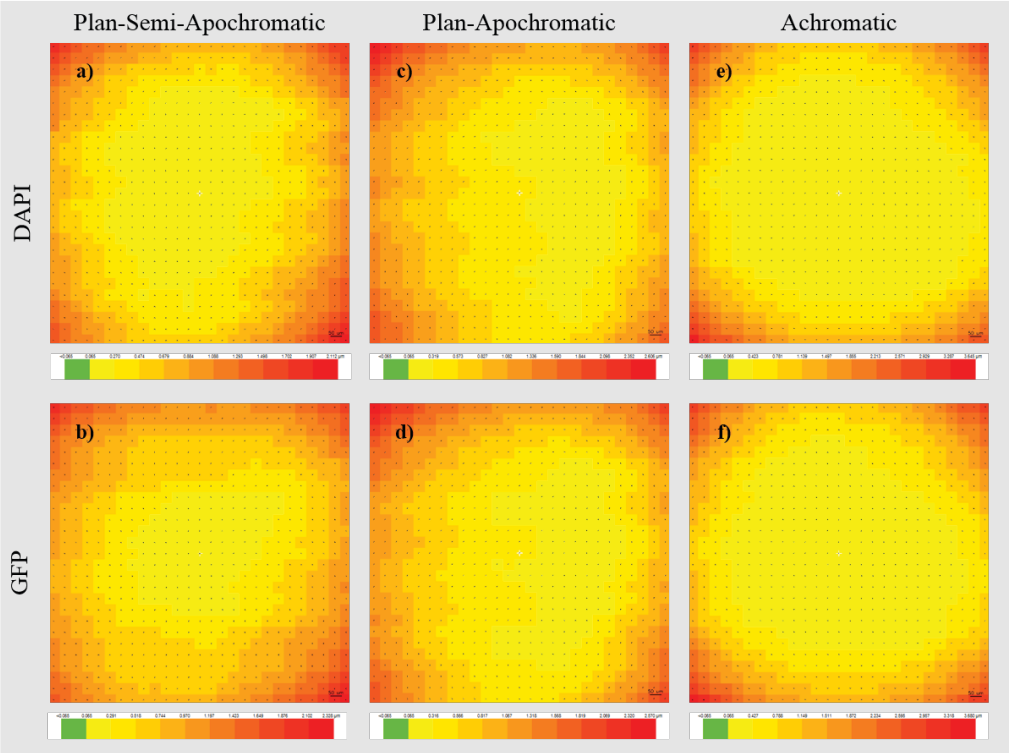

Figure 21: Magnitude and direction heatmaps of the distortion for three different 10× dry objectives, (a, b) Plan-Semi-Apochromatic, (c, d) Plan-Apochromatic, and (e, f) Achromatic, for the DAPI and GFP channels.

	Plan-Semi-Apochromatic		Plan-Apochromatic		Achromatic	
Channel	**DAPI**	**GFP**	**DAPI**	**GFP**	**DAPI**	**GFP**
Mean vector magnitude (µm)	0.56	0.73	0.71	0.71	0.67	0.75
Minimum vector magnitude (µm)	0.06	0.06	0.07	0.07	0.07	0.07
Maximum vector magnitude (µm)	2.11	2.33	2.61	2.57	3.65	3.68
Maximum distortion rate along X (%)	0.15	0.15	0.20	0.20	0.30	0.30
Maximum distortion rate along Y (%)	0.15	0.15	0.15	0.20	0.35	0.35

Table 9: Relevant parameters relative to the distortion of the field of view for the three different 10× dry objectives, DAPI and GFP channels. More information about the meaning and the calculation of these parameters can be found in the documentation of the current version of Daybook.

3.5.3 Color correction

Example

Figure 22 displays the chromatic aberration heatmaps for the three objectives, DAPI with respect to GFP channel.
The relevant parameters associated with chromatic aberrations are gathered in Table 10.

From this figure and table, it can be observed that the Plan-Apochromatic objective presents the lowest maximum chromatic shift. In terms of color correction, if the maximum chromatic shift is the only parameter to consider, the three objectives can therefore be ranked in the following order, from the best to the worst: Plan-Apochromatic, Plan Semi-Apochromatic and Achromatic.

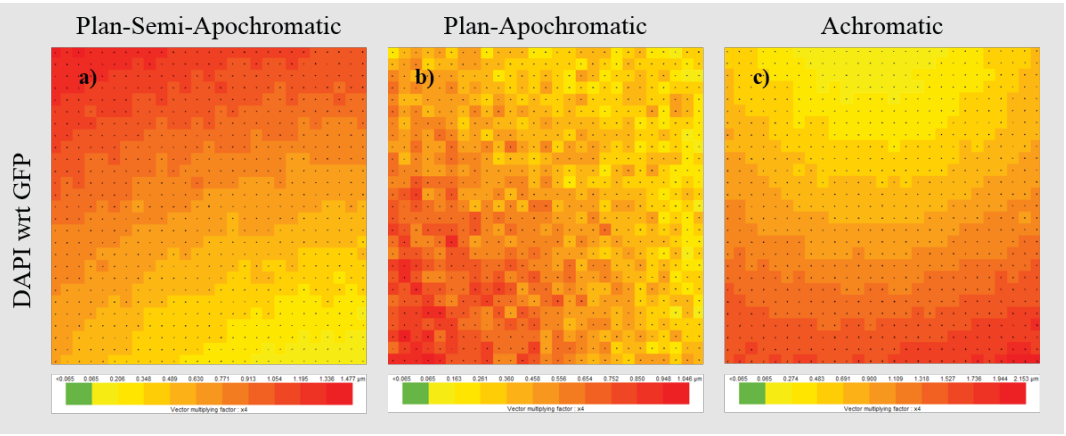

Figure 22: Magnitude and direction heatmaps of the chromatic shifts for three different 10× dry objectives, (a,) Plan-Semi-Apochromatic, (b) Plan-Apochromatic, and (c) Achromatic, DAPI with respect to GFP channel.

	Plan-Semi-Apochromatic	Plan-Apochromatic	Achromatic
Channel	**DAPI wrt GFP**	**DAPI wrt GFP**	**DAPI wrt GFP**
Mean vector magnitude (µm)	0.941	0.892	1.166
Minimum vector magnitude (µm)	0.065	0.065	0.065
Maximum vector magnitude (µm)	1.477	1.046	2.153

Table 10: Relevant parameters relative to the chromatic aberrations for the three different 10× dry objectives, DAPI and GFP channels. More information about the meaning and the calculation of these parameters can be found in the documentation of the current version of Daybook.

3.5.4 Summary

Using a single pattern, the field of rings, it has been possible to compare and rank the performances of three 10× dry objectives in terms of illumination flatness, distortion of the field of view and lateral color correction.

For the tested objectives in this experiment, it has appeared that the Plan-Apochromatic objective (the most expensive one) is better only on the color correction parameter.

If the other parameters (flatness and distortion) are also of importance for the user, and if he/she can lower his/her expectations on color correction, then the Plan-Semi-Apochromatic objective, less expensive, is the best suited.

Other criteria, such as the objectives' PSF, lateral and axial resolving powers, contrast, luminosity, etc., can be added for the comparison. These other criteria may change the objectives ranking and therefore make reconsider the user his/her choice.

4. 4×4 (Argo-HM, -LM and -SIM) and 2×16 (Argo-HM and -SIM) intensity gradations

Note: The intensity gradations should be imaged with a lot of care, in order to preserve their function. It is recommended to read carefully the section "Photostability" in the User Guides.

Figures 23 and 24 show two intensity gradation patterns, either organized in a 4×4 matrix of squares or in a 2×16 matrix of rectangles, imaged on the GFP channel, as well as the evolution of the mean intensity of each square/rectangle versus the level index, from 1 to 16.

Both intensity gradation patterns have the same function. Depending on the illumination inhomogeneity of the microscope, one may prefer to use one or the other.

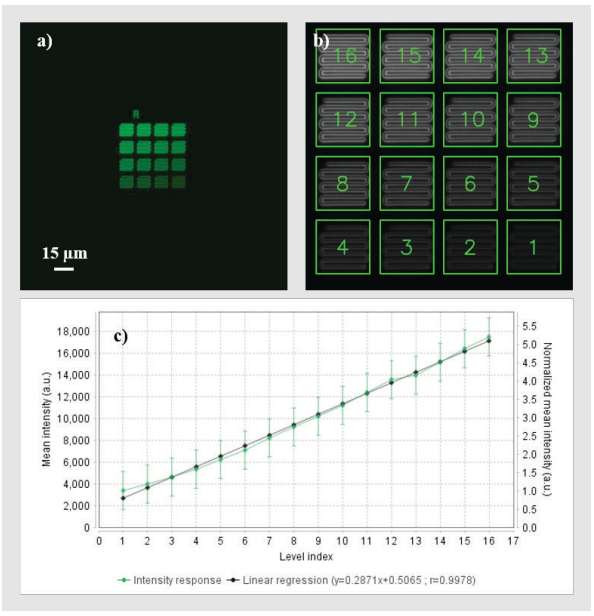

Figure 23: Argo-HM;
(a) Wide-field microscopy image of the 4×4 intensity gradation, acquired with a 63×/1.4 Plan-Apochromat oil objective on the GFP channel.
(b) ROI for each square, from which the mean intensity is extracted.
(c) Evolution of the non-normalized (left axis) and normalized with respect to the first level (right axis) mean intensity of each ROI versus the level index.
The linear regression curve with its equation and the Pearson coefficient of the fit are given.

As insured in the certificate of inspection delivered with each Argo-HM, -LM, or -SIM tool, the 16 intensity levels follow a linear evolution, determined by the fact that the linear regression curve presents a correlation coefficient ≥ 0.98 and passes through all the experimental points having an error bar of ± 10% of the 16th intensity level.

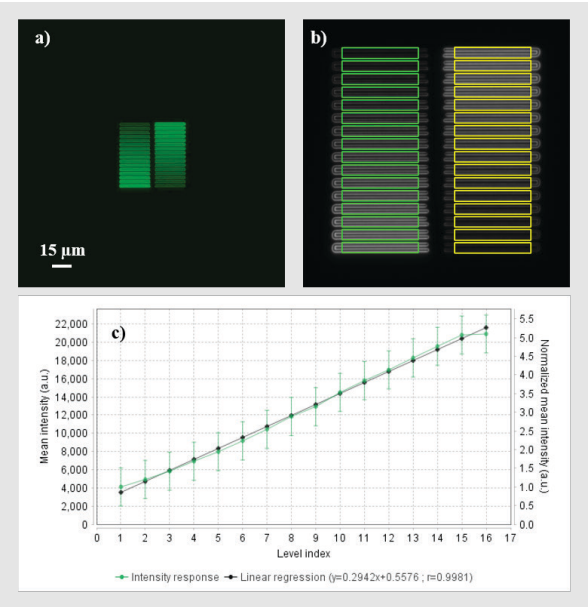

Figure 24: Argo-HM; (a) Wide-field microscopy image of the 2×16 intensity gradation, acquired with a 63×/1.4 Plan-Apochromat oil objective on the GFP channel. (b) ROI for each rectangle, from which the mean intensity is extracted. (c) Evolution of the non-normalized (left axis) and normalized with respect to the first level (right axis) mean intensity of each ROI versus the level index. The linear regression curve with its equation and the Pearson coefficient of the fit are given.

4.1 Overall intensity response

Issue

A decreased intensity response can reflect different problems:

- The insertion of a polarizer in the optical path. This can be identified if the intensity of the newly acquired images is about twice less than usual for the same acquisition parameters.

- The insertion of a DIC (Differential Interference Contrast) slider in the optical path. This can be identified if the intensity of the newly acquired images is about 10% less than usual for the same acquisition parameters.

- A drop-off in sensor's sensitivity, usually due to ageing or over-exposure. This can be identified by using another sensor, if the system is equipped with several, which is typically the case for confocal microscopes.

- A drop-off in light source power and/or light guiding in an optical fiber, usually due to ageing. This can be identified by measuring the optical power of each individual source, if possible just before or after the objective, using a power-meter. If all the installed sources undergo an optical power decrease, then the coupling/alignment all along the optical path should be checked.

- A drop-off in transmission of the fluorescence filters, usually due to ageing. This can be checked by measuring the transmission spectrum of the filters.

Both 4×4 and 2×16 intensity gradations can be used to easily and rapidly check if the overall intensity response of the system stays about the same over time, by acquiring an image with the usual acquisition parameters (light source power, camera exposure time, photomultiplier gain, etc.).

If the usual parameters must be readjusted to obtain an image similar to the previous ones in terms of signal-to-noise ratio and intensity, then the user should question the system, and try to find the origin of the issue.

Example Figure 25 shows confocal microscopy images of the 4×4 intensity gradation, acquired with 5% and 35% laser powers, as well as the evolution of the mean intensity of each square/rectangle versus the level index, from 1 to 16.

Note: The fluctuations of the experimental points around the linear regression curves in the graphs are typical when illumination inhomogeneity is important.

The 5% laser power has been chosen to have the 1st intensity level close to the limit of detection of the system, while the 35% laser power has been chosen to have the 16th level close to the limit of saturation.

The dynamic of the mean intensity normalized with respect to the first level (right axis on the graph) and the slop of the linear regression curve are about the same for both images, *i.e.* about 12 and 0.7 respectively. This is totally different if we consider the mean intensities.

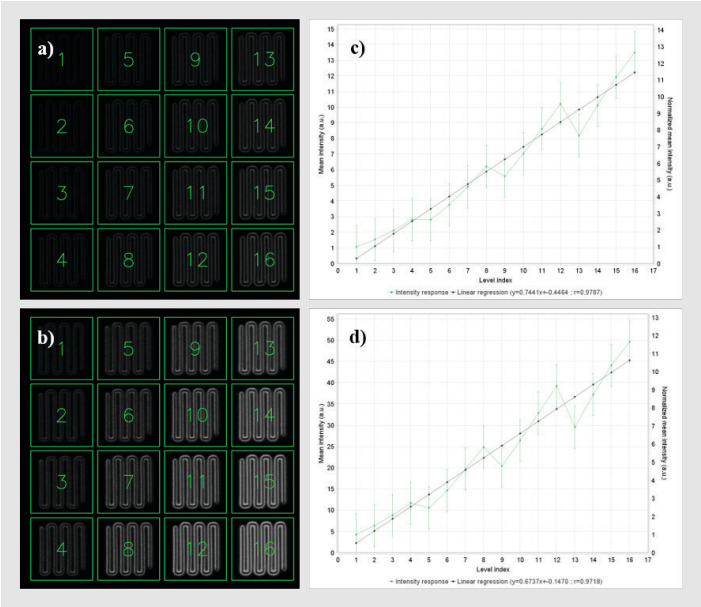

Figure 25: Argo-HM; Confocal microscopy image of the 2×16 intensity gradation, for (a) 5% and (b) 35% laser powers, acquired with a 63×/1.4 Plan-Apochromat oil objective on the GFP channel, zoom magnification of 2, averaged 8 times. The ROI for each square is displayed, from which the mean intensity is extracted. (c, d) Associated evolutions of the non-normalized (left axis) and normalized with respect to the first level (right axis) mean intensity of each ROI versus the level index. The linear regression curve with its equation and the Pearson coefficient of the fit are given. Note that the fluctuations of the experimental points around the linear regression curves in the graphs are typical when illumination inhomogeneity is important.

Example Figure 26 displays the evolution of the absolute mean intensity of each square versus the level index and their associated linear regression curves, for the 4×4 intensity gradation imaged with 5, 10, 15, 20, 25, 30 et 35% laser powers.

Although for 5, 10, 15 and 20% laser powers, the slope of the linear regression curve increases constantly, it appears that for 25, 30 and 35% laser powers, the linear regression curves superimpose.

This tends to indicate that there is a malfunction of the laser power adjustment, which saturates above 20%. Complementary measurements using an optical power-meter should be carried out to confirm this hypothesis.

This is a typical example which illustrates the fact that, when an issue in the intensity response is detected, it is mandatory to use a power-meter to identify and dissociate the origin of the problem: from the excitation (laser power and coupling, filters transmission, AOTF, etc.) or the emission (sensor sensitivity, filters transmission, etc.) paths of the system.

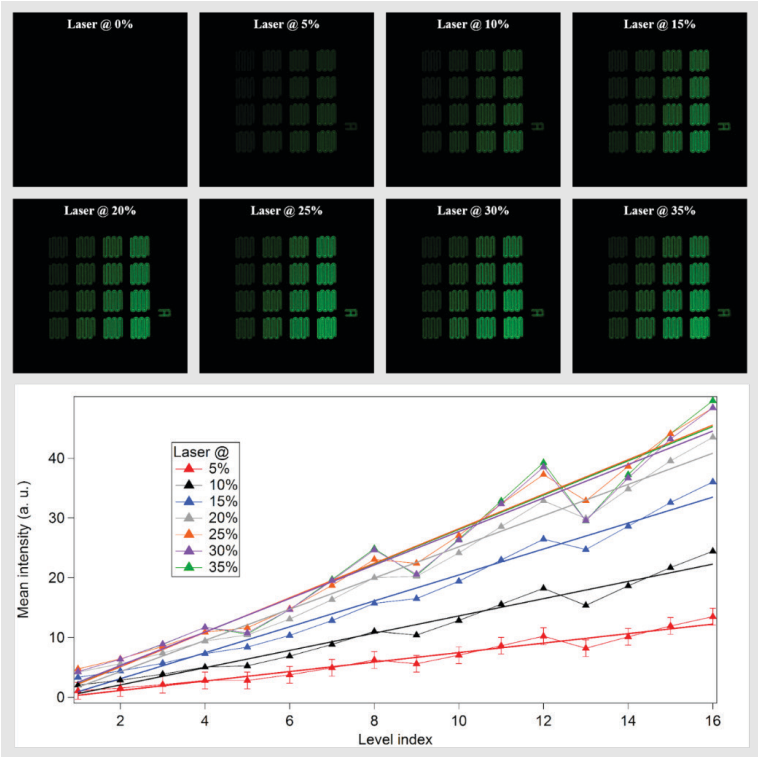

Figure 26: Evolution of the absolute mean intensity of each square versus the level index and their associated linear regression curves, for the 4×4 intensity gradation imaged with 5, 10, 15, 20, 25, 30 et 35% laser powers.

4.2 Evolution of the intensity response

Issue The overall intensity response of fluorescence microscopes may evolve over time, especially on confocal microscopes, and widefield microscopes equipped with metal-halide illuminators.

Example Researchers at the Friedrich Miescher Institute for Biomedical Research (Basel, Switzerland) monitored the intensity response of a widefield fluorescence microscope equipped with a metal-halide illuminator for nearly five months using an Argo-HM (*cf.* Figure 27).

The research team has measured fluctuations of ±15%, clearly illustrating changes in the intensity response of the device, from either its illumination components (light source, filter) or its detection assembly (camera, filter).

Most likely, as it is well known [7], the matters come from the output power of the metal-halide illuminators, which fluctuates over time.

Because of their complexity, intensity fluctuations of laser-scanning microscopes can be of the same order of magnitude.

For the cell or developmental biologist who wants to perform a study over time, if the intensity of the images is meant to be used, it is necessary to normalize them with respect to the intensity response of the system.

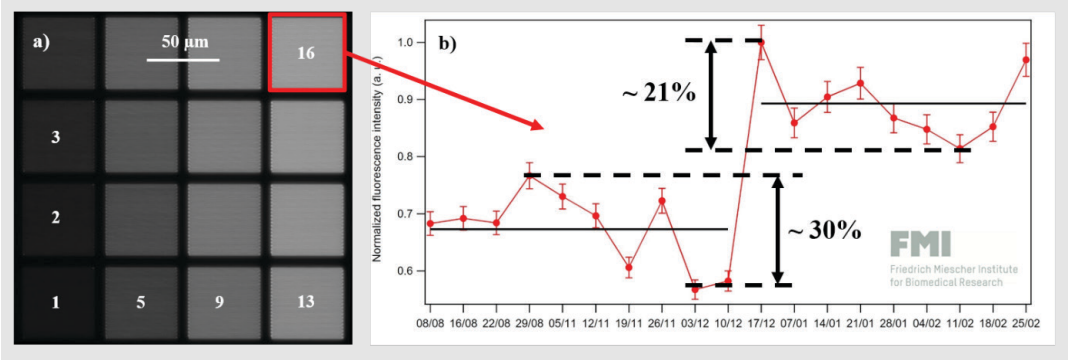

Figure 27: (a) Wide-field microscopy image of the 4×4 intensity gradation pattern from a widefield microscope [ZEISS Axio Imager Z1, Objective Plan-Apochromat dry 20×/0.8, Filter set #10 (Exc: 450–490 nm, BS: 495 nm, Em: 500-550 nm), Metal-halide X-Cite 120 illumination, Cameras Axiocam MRm until 12/10/2014, then Axiocam 506 from 12/17/2014]. (b) Evolution of the 16th square intensity over time with the same settings applied for each measurement. The jump from 12/10/2014 to 12/17/2014 corresponds to the change of the camera (b). Images acquired by Ivana Horvathova and Laurent Gelman at the Friedrich Miescher Institute for Biomedical Research.

4.3 Comparison of cameras' performances

Issue The choice of the camera for a given application in life sciences depends on its performances: speed, sensitivity, linearity, dynamics, noise, etc.

Both 4×4 and 2×16 intensity gradations can be used to compare camera performances, between different technologies (CCD, CMOS and EMCCD), in terms of linearity range, detection and saturation limits, signal-to-noise ratio, etc.

5. Gradually spaced lines (Argo-HM and -SIM)

5.1 Lateral resolving power

The lateral resolving power is the ability of a microscope to resolve two objects close from each other with a defined contrast.

Issue

In any fluorescence microscope, a degradation of the lateral resolving power induces a loss of contrast in sample images.

Many aspects can modify the system's PSF and therefore its lateral resolving power. Non-exhaustively, they are:

- the insertion of a DIC (Differential Interference Contrast) slider in the optical path,
- the dirt on a microscope objective,
- the damaging of a microscope objective,
- the use of an immersion medium with an inappropriate refractive index, introducing additional spherical aberrations.

Pairs of lines, separated by a gradually increasing spacing, and oriented in different directions, allows to determine the lateral resolving power.

Example

Figures 28 and 29 display wide-field images of vertical and 45°-oriented gradually spaced lines acquired with a 63×/1.4 Plan-Apochromat oil objective, for the DAPI and GFP channels, respectively.

After processing these images, Daybook delivers the intensity line profile perpendicular to the gradually spaced lines, from which is extracted the pseudo modulation transfer function (MTF).

The usual MTF is the evolution of the contrast (or modulation) versus spatial frequencies for several imaged periodic square structures having different periods. Here, the pseudo MTF is the evolution of the contrast versus the line spacing (in the real space).

From the pseudo MTFs shown in Figures 28 and 29, the lateral resolving power for a chosen contrast value (here 15%) can be extracted. For the vertical lines, the measured resolving powers are 0.31 and 0.38 µm for the DAPI and GFP channels, respectively, while for the 45°-oriented lines, they are 0.34 and 0.36 µm.

As expected, the resolving power is better for the DAPI channel than for the GFP one, for both lines orientations. It also varies with the lines orientations, because of the arrangement of the camera pixels into an array.

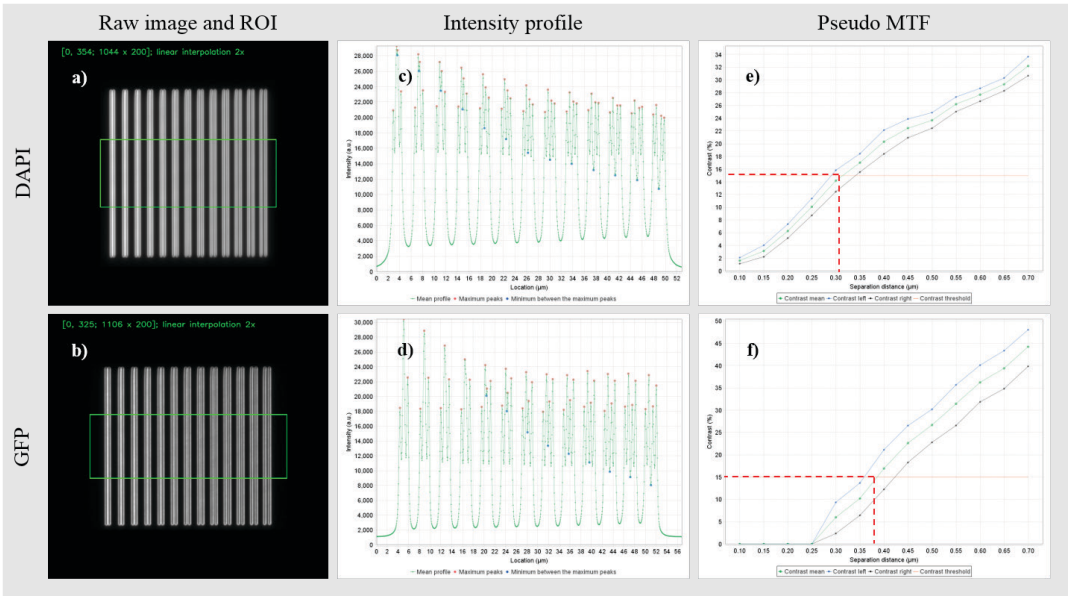

Figure 28: Argo-HM; (a, b) Wide-field microscopy images of the vertical gradually spaced lines, acquired with a 63×/1.4 Plan-Apochromat oil objective on the DAPI and GFP channels. (c, d) Intensity profiles associated to the ROI in the raw images. (e, f) Pseudo modulation transfer function. The measured resolving powers for a defined contrast of 15% are 0.31 and 0.38 µm for the DAPI and GFP channels, respectively. As expected, the resolving power is better for the DAPI channel than for the GFP one.

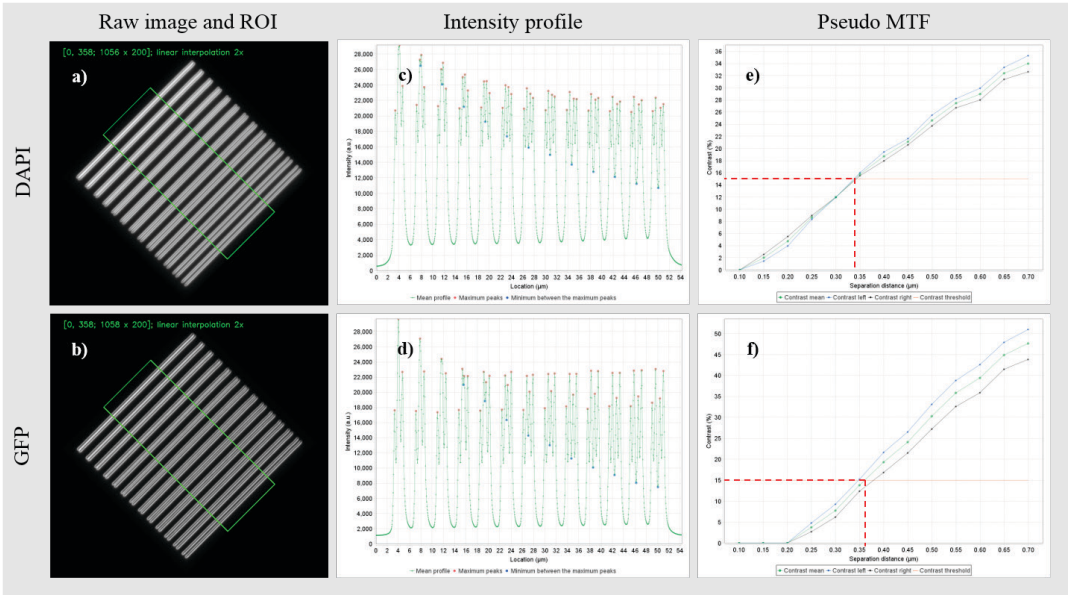

Figure 29: Argo-HM; (a, b) Wide-field microscopy images of the 45°-oriented gradually spaced lines, acquired with a 63×/1.4 Plan-Apochromat oil objective on the DAPI and GFP channels. (c, d) Intensity profiles associated to the ROI in the raw images. (e, f) Pseudo modulation transfer function. The measured resolving powers for a defined contrast of 15% are 0.34 and 0.36 µm for the DAPI and GFP channels, respectively. As expected, the resolving power is better for the DAPI channel than for the GFP one.

5.2 Lateral resolving power versus pinhole size

Issue

Fluorescence confocal microscopes allow an improvement in the lateral resolving power with respect to that of conventional microscopes when decreasing the pinhole diameter below 1 Airy unit (au).

This improvement can be directly observed and checked thanks to the gradually spaced lines, thus validating the theoretical expectations.

Example

Figure 30 shows the evolution of the lateral resolving power for different pinhole sizes. The lateral resolving power decreases from 0.28 down to 0.20 µm when decreasing the pinhole diameter from 1 to 0.25 au. This is consistent with the theoretical expectations.

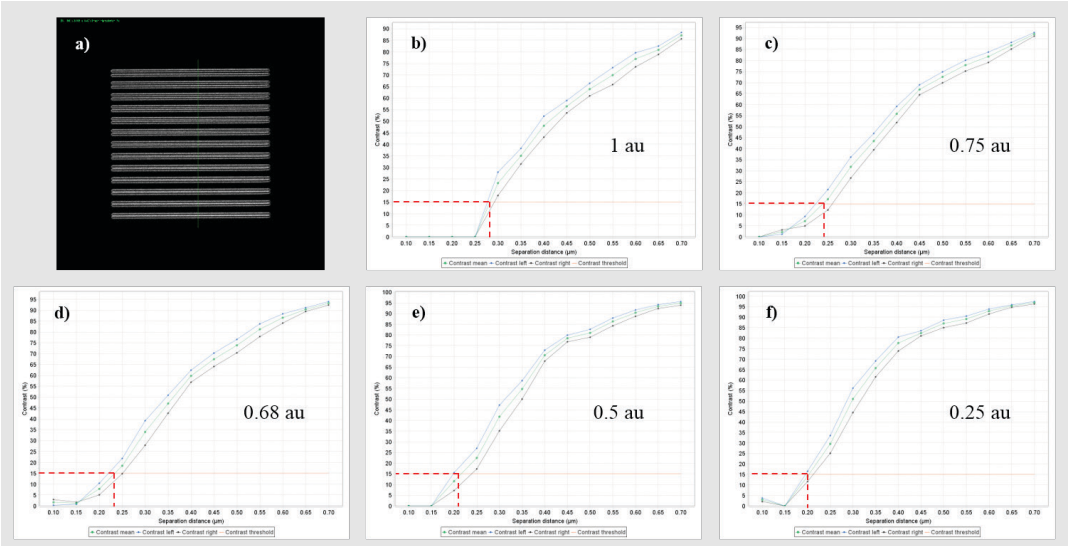

Figure 30: Argo-HM; (a) Example of confocal microscopy images of the horizontal gradually spaced lines, acquired with a 40×/1.3 Plan-Apochromat oil objective on the GFP channel. Pseudo modulation transfer functions for different pinhole diameters: (b) 1 Airy unit (au), (c) 0.75 au, (d) 0.68 au, (e) 0.5 au and (f) 0.25 au. The measured resolving powers for a defined contrast of 15% are 0.28, 0.24, 0.23, 0.21 and 0.20 µm for 1, 0.75, 0.68, 0.5 and 0.25 au pinhole diameters. As expected, the resolving power decreases with the pinhole diameter.

5.3 Comparison of different methods

Issue

The knowledge of resolution improvement obtained from different imaging methods is often of importance in the process of choosing a method for a particular life sciences application.

Gradually spaced lines can be used to compare the performances of conventional images deconvolution with respect to super-resolution microscopy.

Example Figure 31 shows images acquired with a wide-field microscope, deconvolved images, and images acquired with a structured illumination microscope (SIM).

In this example, as expected, the comparison shows a better resolving power for SIM than for deconvolution and wide-field imaging.

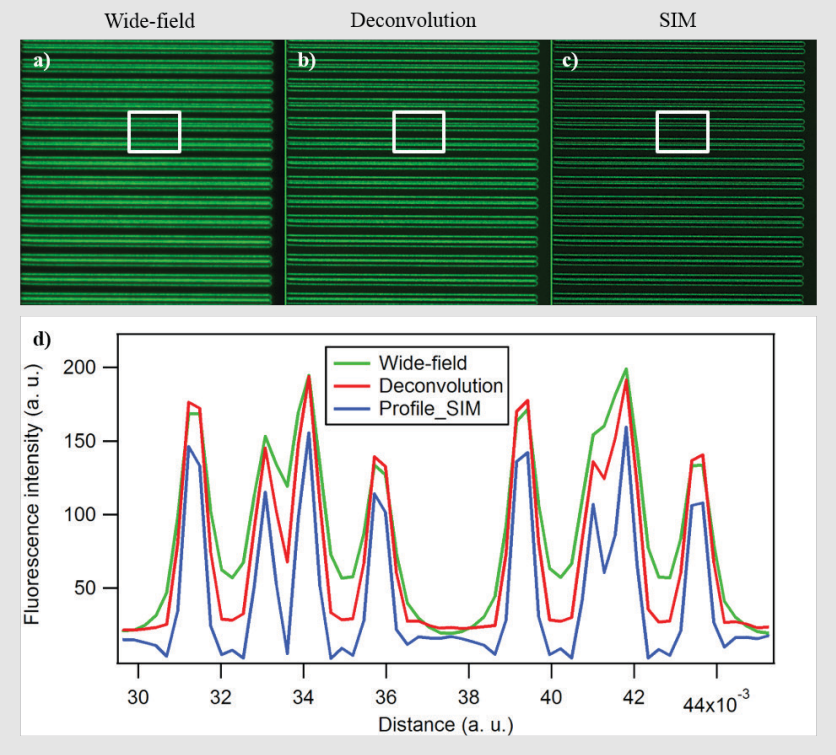

Figure 31: Argo-SIM; (a) Wide-field microscopy, (b) deconvolved and (c) structured illumination microscopy image of the horizontal gradually spaced lines, acquired with a 63×/1.4 Plan-Apochromat oil objective on the GFP channel. (d) Intensity profiles perpendicular to the lines from the white frame for each imaging method. As expected, the comparison shows a better resolving power for SIM. Images acquired by Uri Manor, Waitt Advanced Biophotonics Core Facility, Salk Institute for Biological Studies.

6. Matrix of crosses (Argo-HM and -SIM)

6.1 Axial resolving power

The axial resolving power is the ability of a microscope to resolve two objects on top of each other with a defined contrast.

Issue In any fluorescence microscope, a degradation of the axial resolving power induces a loss of contrast in sample images. Many aspects can modify the system's PSF and therefore its axial resolving power, in such a way that is much more pronounced than for the lateral resolving power.

Non-exhaustively, they are:

- the insertion of a DIC (Differential Interference Contrast) slider in the optical path,
- the dirt on a microscope objective,
- the damaging of a microscope objective,
- the use of an immersion medium with an inappropriate refractive index, introducing additional spherical aberrations.

Example The crosses in the matrix are made of vertical lines in the same XY plane, and of horizontal lines that go deeper and deeper in the glass.

For a user-defined contrast, one can measure the distance between the horizontal and vertical lines forming a single cross for which he/she considers they are axially resolved, as it is illustrated in Figure 32.

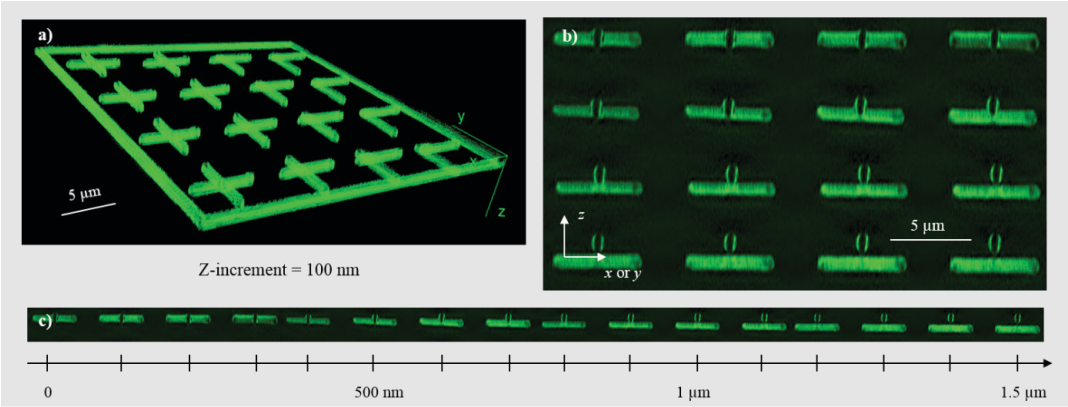

Figure 32: Argo-SIM; (a) 3D reconstruction and (b, c) 2D montages of the matrix of crosses acquired with a structured illumination microscope, 63×/1.4 Plan-Apochromat oil objective on the GFP channel. Images acquired by Talley Lambert, Cell Biology Microscopy Facility, Harvard Medical School.

7. Meridians of a sphere (Argo-HM and -SIM)

7.1 3D reconstruction accuracy

Issue One of the biggest advantages of laser-scanning microscopes is their ability to acquire image slices of a sample by filtering the out-of-focus light, so that its reconstruction and visualization is possible.

Assessing the optical sectioning and Z-stacking capabilities of such microscopes is therefore important.

3D fluorescent patterns with well-known shape and dimensions, such as the meridians of a sphere, are perfectly suited for this purpose. Thus, any stage drift during the Z-stacking can easily be identified after 3D reconstruction.

Example Figure 33 shows an accurate 3D reconstruction of the meridians of the sphere in an Argo-HM from a Z-stack of confocal microscopy images.

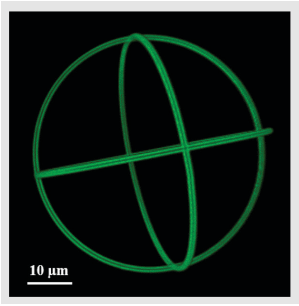

Figure 33: Argo-HM;
3D reconstruction of the meridians of a sphere from a Z-stack of confocal microscopy images acquired with a 63×/1.4 Plan-Apochromat oil objective on the GFP channel.

7.2 Z-distance

Issue Z-distances displayed by the acquisition software of fluorescence microscopes may be inaccurate, as they rely on the Z-stage precision and depend on the refractive index of the sample and of the immersion medium.

The meridians of the sphere in the Argo-HM are circles with a diameter of 50 µm, in the XY, XZ and YZ planes.

The measurement of the diameters of the circles in the XZ and YZ planes allows to check if the Z-distances provided by the microscope acquisition software are accurate.

Example Figure 34 shows the XY, YZ and XZ orthogonal views of the sphere meridians from a Z-stack of confocal microscopy images. The measured diameter of the sphere in the Z-direction is 49.9 µm, which is in accordance with the 50 µm announced.

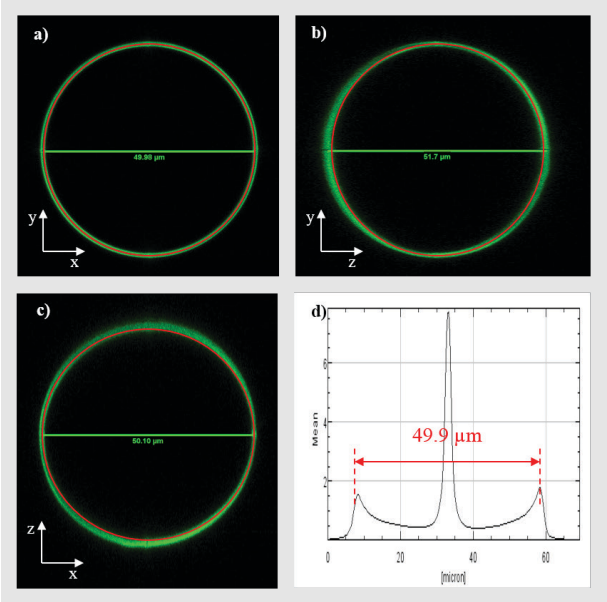

Figure 34: Argo-HM;
(a) XY, (b) YZ and (c) XZ orthogonal views of the sphere meridians from a Z-stack of confocal microscopy images acquired with a 63×/1.4 Plan-Apochromat oil objective on the GFP channel. (d) Mean intensity of the entire stack versus the Z distance. The red circles on top of the orthogonal views are perfect circles, and are displayed for information.

In the present experiment, an oil objective was used. When using a dry objective, the measurement of the diameter of the sphere in the Z-direction is reduced by a factor corresponding to the refractive index difference between the glass and the air, *i.e.* about 1.523.

A correction is therefore necessary to get back to the actual value of the axial diameter of the sphere. Most microscope acquisition softwares include this possibility.

8. Crossing stairs (Argo-HM, -LM and -SIM)

8.1 3D reconstruction accuracy

Issue

As for the meridians of the sphere, the 3D crossing stairs can be used to assess the optical sectioning and Z-stacking capabilities of laser-scanning microscopes, as it is illustrated in Figure 35.

Thus, any stage drift during the Z-stacking can easily be identified after 3D reconstruction.

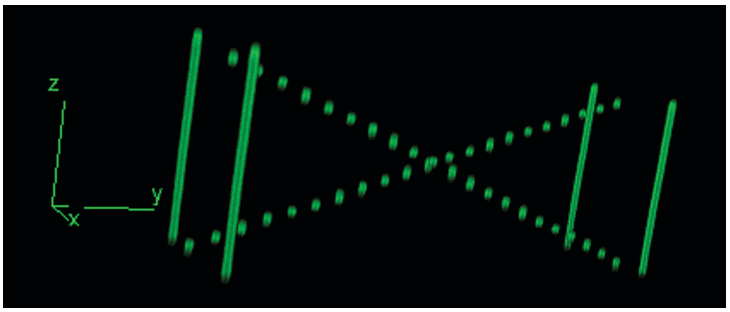

Figure 35: Argo-HM; 3D reconstruction of crossing stairs from a Z-stack of confocal microscopy images acquired with a 63×/1.4 Plan-Apochromat oil objective on the GFP channel.

8.2 Z-stage drift

Issue

The environmental conditions around a fluorescence microscope can influence its performances. This is even more true if high resolution and/or precision are required for a given experiment. In particular, the axial drift of microscope stages is very sensitive to temperature and air flow fluctuations.

It is difficult to appreciate the amount of drift there would be during a long imaging session. Usually, it is required to acquire several Z-stacks to know about the Z-stage drift.

Here, from the acquisition of 2D images, containing a 3D information, it is possible to measure this parameter.

Example Figure 36 shows 2D images of the 0.75 µm step stairs. Initially, the focusing is performed in the middle of the stairs. A continuous drift, up to four steps (that is 4 × 0.75 µm = 3 µm) can be noticed after some time.

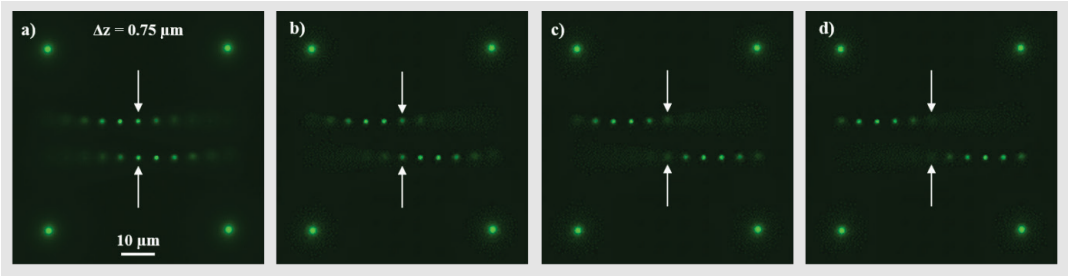

Figure 36: Argo-HM; (a-d) 2D confocal microscopy images of the 0.75 µm step crossing stairs, acquired at different time intervals with a 63×/1.4 Plan-Apochromat oil objective on the GFP channel, open pinhole. The focusing plane has drifted after some time, as it is evidenced by the arrows indicating the initial stair steps in focus.

7.3 Objectives' optical aberrations

Issue Optical aberrations, such as astigmatism or spherical aberration, can be identified in fluorescence microscopy by acquiring a Z-stack of images in the XY plane (or single images in the XZ or YZ planes) of fluorescent beads or any fluorescent object having a sufficiently small axial extension.

The signature of both these aberrations is much more pronounced in the axial direction. That is why the acquisition of a 2D image in the XY plane of such samples should not bring much information on their presence and magnitude.

Acquiring a 2D image of the stairs in the Argo-tools provides a 3D information, as the steps are at well-defined depths inside the glass.

The out-of-focus steps spread the light in a way that depends on the quality of the optical components (mainly the objective) and the alignment of the microscope.

Uncircular spreading is characteristic of astigmatism, while asymmetric spreading on each side of the focal plane is typical of spherical aberrations.

Example Figure 37 displays confocal images with different gamma values of crossing stairs. They have been acquired with a 1 Airy unit pinhole diameter.

For the objective without astigmatism, the images show circular light spreading. For the objective presenting some astigmatism, the images show uncircular (oval) spreading, signature of astigmatism. The effect looks more pronounced when the gamma parameter is set to 0.45.

The same approach can be used to identify spherical aberration, objective damage or the presence of a DIC slider in the optical path.

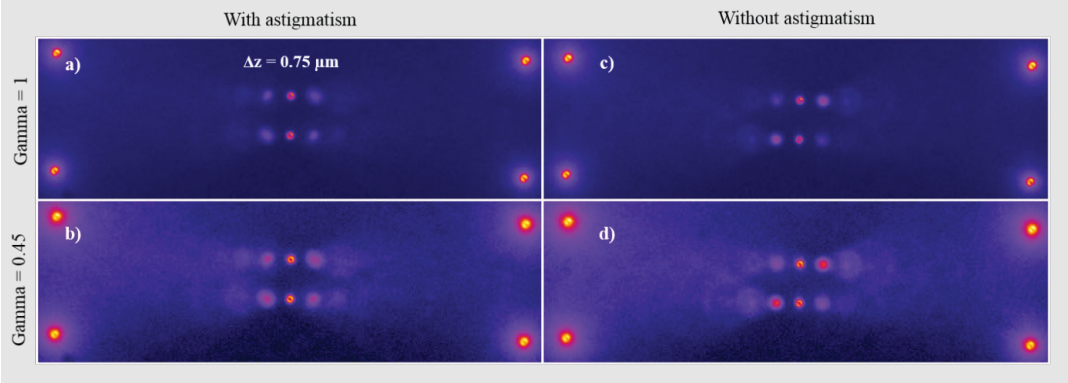

Figure 37: Argo-HM; 2D confocal microscopy images of the 0.75 µm step crossing stairs, acquired on the GFP channel with two 63×/1.4 Plan-Apochromat oil objectives of the same model, (a, b) with an objective presenting some astigmatism and (c, d) with an objective presenting no astigmatism. The astigmatism is evidenced by the uncircular light spreading from the out-of-focus stair steps. The effect looks more pronounced when the gamma parameter is set to 0.45. Images acquired by Laurent Gelman at the Friedrich Miescher Institute for Biomedical Research.

9. Repositioning crosses (Argo-HM, -LM and -SIM)

9.1 Stage repositioning accuracy

Issue

Stage repositioning accuracy is of importance for stitching of images. Manufacturers provide a repositioning error associated to the stages.

It can easily be checked as follows:

- center a well-defined object in the center of the field of view (a cross for example),
- move the sample back and forth in different directions,
- acquire images each time the sample comes back to its initial position.

Superposing the images and detecting the centroid of the object of interest in each image allows to determine the spatial shift after each round trip, and to check if the shift is within the specifications.

Example

Figure 38 displays the superposition of images of a fluorescent cross after round trips in the X and Y directions.

One can observe on the virtual target that the stage repositioning accuracy is higher than the manufacturer specification, *i.e.* 5 µm.

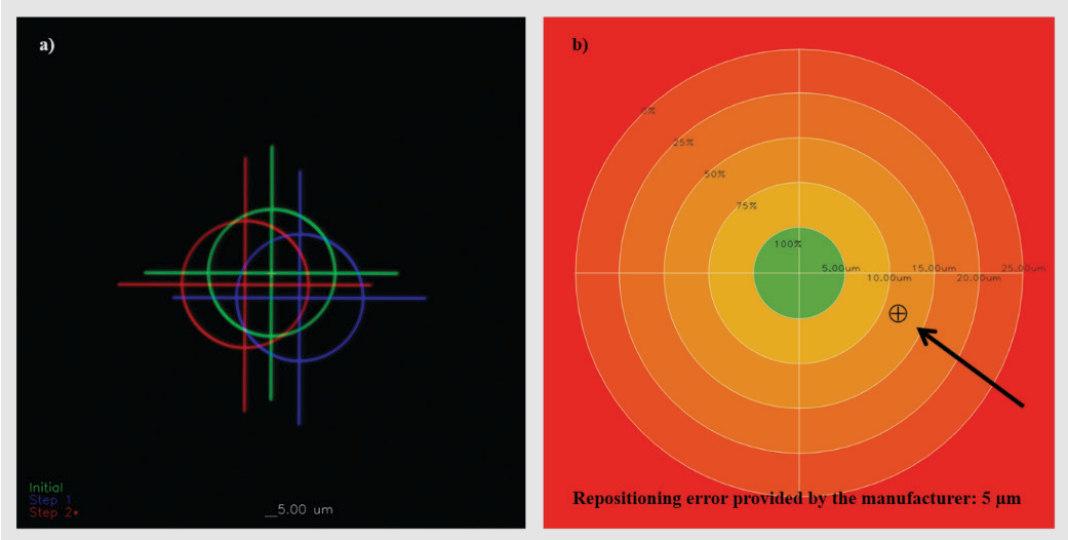

Figure 38: (a) Superposition of images of a fluorescent cross after round trips in the X and Y directions. (b) Repositioning position on a virtual target, showing the experimentally determined accuracy compared to the value given by the manufacturer.

9.2 Objectives issues

Issue

The presence of dust or dried oil on the front lens of an objective, or its damaging (due to scratches or hits) can dramatically alter image quality.

For this reason, it is highly recommended, before starting any imaging session, to check if an objective present such issues.

A simple and quick way to perform this inspection is to look at a fluorescent cross through the eyepiece and to change the focusing on both sides of the object plane. Of course, this application depends on the user's experience, but after some time using the Argolight tools, one might rapidly identify these problems.

Example

Figure 39 displays XY and XZ orthogonal views from a Z-stack of a fluorescent cross. The 63×/1.4 Plan-Apochromat oil objective had dirt (dried oil or dust) on its front lens, and has been cleaned afterwards.

The presence of dirt is evidenced by a blurrier XY image and a larger Z-extension. This simple test can provide information on the cleanliness of the objective.

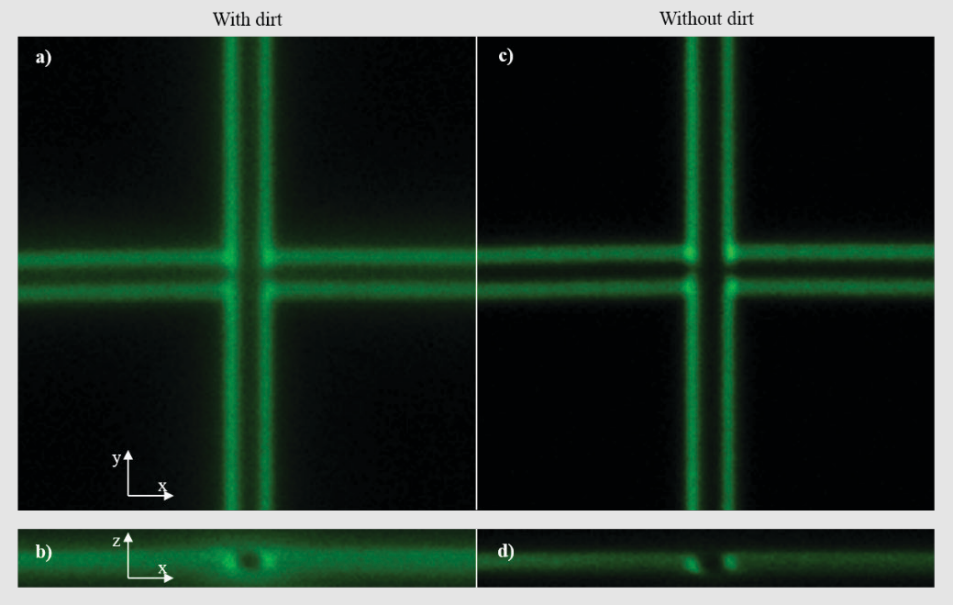

Figure 39: Argo-HM; (a, c) XY and (b, d) XZ views of a cross from a Z-stack of confocal microscopy images acquired with a 63×/1.4 Plan-Apochromat oil objectives, (a, b) with dirt on the front lens and (c, d) with the dried oil cleaned. The presence of dried oil is evidenced by a blurrier XY image and a larger Z-extension. Images acquired by and Laurent Gelman at the Friedrich Miescher Institute for Biomedical Research.

10. Logo (Argo-HM, -LM and -SIM)

10.1 Rotated or mirrored image

Issue

Because the Argolight logo has an asymmetric shape, it can be used to check if a camera or the scanning is well-oriented with respect to the microscope stages, or if there is a lens in the optical path that modifies the image.

If the word ARGOLIGHT cannot be read horizontally in the image, this is the signature of camera or scanning mis-orientation.

If the word ARGOLIGHT is read in a mirrored way in the image, this is the signature of the presence of a lens in the optical path that reverses the image.

10.2 System's spectral response

Issue

Fluorescence microscopes, although conceived preliminary to be imaging systems, can also acquire emission spectra, with a better spatial resolution but poorer spectral resolution than conventional spectrometers.

Correct interpretation of emission spectra measured with a microscope requires the knowledge of its spectral response.

The fluorescence emission spectra of the patterns have been measured internally using a calibrated conventional spectrometer. Those “true” spectra are stored in Daybook’s database.

Any emission spectrum measured with a microscope can therefore be compared to the true spectrum through Daybook, which determines the spectral response of the microscope, *i.e.* the ratio of the measured spectrum by the true one.

A perfect spectral response should be flat in the entire collection spectral window.

Example

Figure 40 displays the emission spectrum measured with a confocal microscope, the true spectrum measured with a calibrated spectrometer, and the spectral response of the system for a 488 nm excitation wavelength and 510-650 nm collection window.

Results show variations of about 20% in the system spectral response. This means that spectra measured with this system can present deviations of this amount in the true normalized emission intensity.

Such a method can also be applied to assess or follow the transmission features of fluorescence filters.

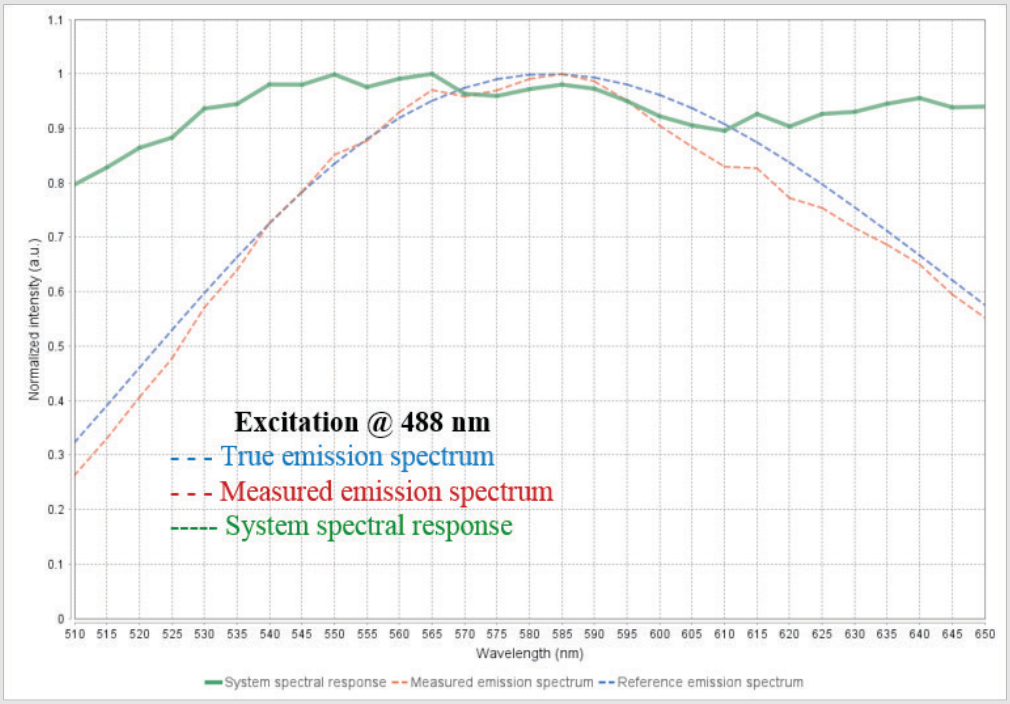

Figure 40: True (in blue) and measured (in red) normalized emission spectra of the patterns for a 488 nm excitation wavelength. The system spectral response (in green) is the ration of the measured spectrum by the true one

10.3 Evolution of the system's time response

Issue

The fluorescence of the patterns presents short lifetimes. They can therefore be used to assess the time response evolution of Fluorescence Lifetime Imaging Microscopes (FLIM).

The fluorescence decay can typically be fitted by a bi-exponential function. The values of the decay rates are in the range of the sub-nanosecond (ns) for the short component, and in the range of a few ns for the longest one.

These values are subject to change, depending on the excitation wavelength and collection spectral window set during the acquisition, but remain in these orders of magnitude.

Therefore, rather than determining the absolute response time of a FLIM, such decay curves can be used to follow its evolution.

Example

Figure 41 shows a typical fluorescence lifetime, with extracted decay rates of about 0.3 and 2.5 ns.

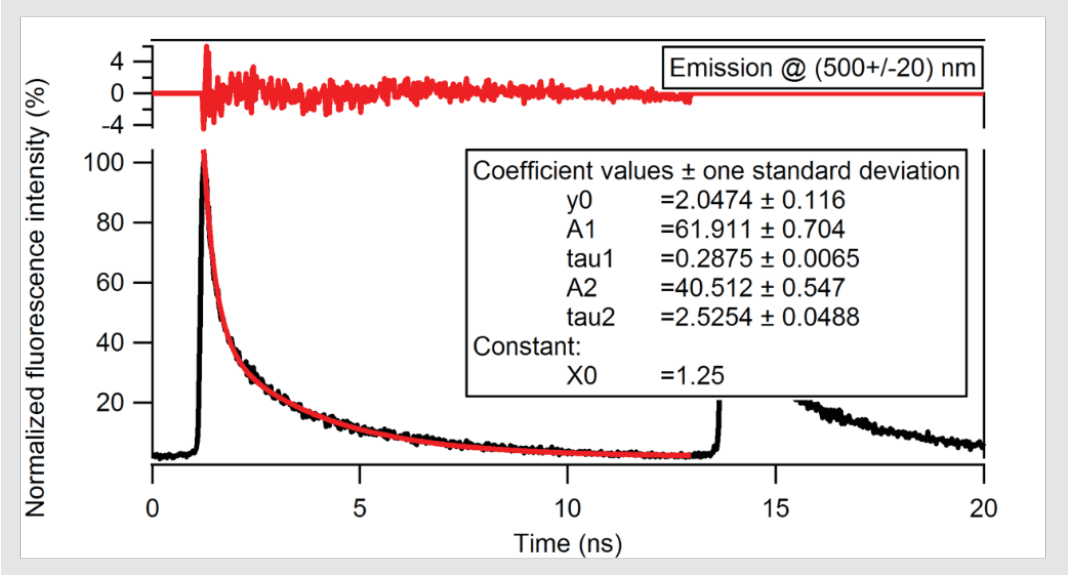

Figure 41: Typical fluorescence lifetime of the patterns [λexc = 400 nm, Δλem = 500±20 nm, 10×/0.25]. A bi-exponential function has been used to fit the decay experimental data, which residual is shown on top. The decay has two components: one at about 0.3 ns, and another one at 2.5 ns.

11. Geometrical figures (Argo-SIM)

Issue

Some imaging techniques, such as structured illumination microscopy (SIM), require the use of specialized algorithms to get a reconstructed super-resolution image from a set of raw images.

However, these specialized algorithms can introduce artifacts in the reconstructed image, depending on the signal-to-noise ratio of the raw images [8].
The geometrical figures allow to assess the accuracy of SIM reconstruction algorithms, and to observe the artifacts they may introduce.

Example Figure 42 shows normalized images of a 16-arms star and a heptagon acquired with a SIM.

Clear artifacts can be observed from the reconstruction between the arms of the star, as well as inside the heptagon.

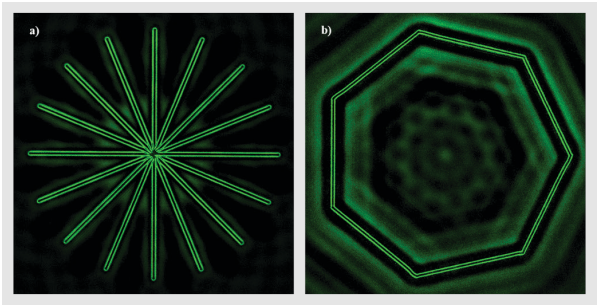

Figure 42: Argo-SIM; Structured illumination microscopy of a 16-arms star and a heptagon acquired with a 63×/1.4 Plan-Apochromat oil objective on the GFP channel. Reconstruction algorithms artifacts can be observed. Images acquired by Talley Lambert, Cell Biology Microscopy Facility, Harvard Medical School.

12. 3D matrix of rings (Argo-SIM)

Issue In the same way as the 2D field of rings, the 3D matrix of rings can be used to assess the same aspects, but in a much larger volume, in particular axial chromatic shifts and deconvolution performance.

This last aspect is illustrated in Figure 43, which shows the deconvolution of a Z-stack of wide-field images.

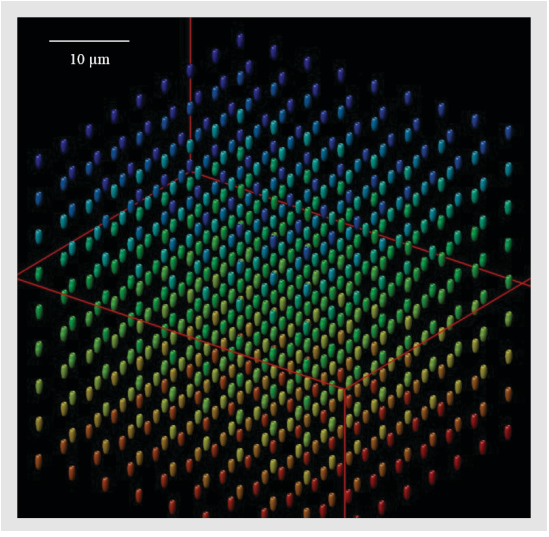

Figure 43: Deconvolution of a Z-stack of wide-field images of the 3D matrix of rings, acquired with a 63×/1.4 Plan-Apochromat oil objective on the GFP channel. The color coding refers to the depth of the rings.

Images were deconvolved and (MIP/surface) rendered using the Huygens Professional software (www.svi.nl).

13. Frequently Asked Questions

12.1. Any doubt from the Argolight tools?

While using the Argolight tools, you may at some point question the reality of observed effects, whether they come from the imaging system or from a defect in the product. Any Argolight product is delivered with a User Guide and a Certificate of Inspection which ensures that the slide is free of defect, as each pattern and most of the aspects are checked and documented.

12.2. Lateral chromatic shifts

If a lateral chromatic shift is observed between two channels in one direction, and if the reality of this shift is questioned, then the user can acquire an image of the Argolight logo, rotate physically the tool by 180°, and re-acquire an image of the Argolight logo. If the lateral chromatic shift is still observed in the same direction, then the problem comes from the system. This approach can be generalized to other issues.

12.3. Blurred image

If a blurred image of one or several patterns is observed, then the user can question the cleanliness of either the tool or the microscope objective. Please read the section “Cleaning” in the User Guides to solve this issue.

12.4. Low fluorescence emission intensity

If a lower fluorescence emission intensity than usual is observed, we recommend to check all the aspects listed in the section 3.1 of this document to identify the origin of this issue.

12.5. Patterns hard to find

As the patterns have a low thickness (from a few µm to a few hundreds of nm) and present a relatively low brightness, it can be difficult to find them. Please read the section “Starting procedure” in the User Guides to solve this issue.

References

[1] A. Dixon, T. Heinlein and R. Wolleschensky, “Standardization and quality assurance in fluorescence measurements II,” Chapter 1, Springer-Verlag, Berlin Heidelberg (2008).

[2] J. Pawley, “The 39 Steps: A cautionary tale of quantitative 3-D fluorescence microscopy,” Biotechniques 28, 884-886 (2000).

[3] J. C. Waters, “Accuracy and precision in quantitative fluorescence microscopy”, The Journal of Cell Biology, 185, 1135-1148 (2009).

[4] U. Resch-Genger, K. Hoffmann, W. Nietfeld, A. Engel, J. Neukammer, R. Nitschke, B. Ebert, and R. Macdonald, “How to improve quality assurance in fluorometry: Fluorescence-inherent sources of error and suited fluorescence standards,” Journal of Fluorescence 15, 337-362 (2005).

[5] http://zeiss-campus.magnet.fsu.edu/articles/basics/objectives.html

[6] H. Beyer, “Handbuch der mikroskopie,” 2nd Edition, VEB Verlag Technik Berlin (1985).

[7] T. R. Baird, D. Kaufman, and C. M. Brown, “Mercury free microscopy: An opportunity for core facility directors,” Journal of Biomolecular Techniques 25, 48-53 (2014).

[8] T. J. Lambert and J. C. Waters, “Navigating challenges in the application of super-resolution microscopy,” Journal of Cell Biology, DOI: 10.1083/jcb.201610011 (2016).

Date of issue
01/04/2017

Version
1.0

Author
Arnaud Royon, Ph.D.
Chief Technical Officer and Co-founder

Contact information
Argolight SA
11 Avenue de Canteranne
Bat. Elnath
33600 PESSAC
FRANCE
sav@argolight.fr
www.argolight.com

Note for readers
The experimental data shown in this documentation are informative and not contractual, and may be different from one system to another.

Disclaimer
To the extent allowed by law, Argolight will not be liable for special, incidental, indirect, punitive, multiple or consequential damages in connection with or arising from this document, including the use of it.

A word about waste management
Argolight policy is to offer robust products that last.

In the event our products become useless to you, please contact us so we can pick them up and recycle them.
Please do not throw away the slide with common waste.
The composition of the glass requires specific recycling. Thank you.

www.argolight.com

For support visit www.argolight.com
or email sav@argolight.fr

ARGOLIGHT
A Precision Company